EC
Journals.ASM.org

The Contribution of *Candida albicans* Vacuolar ATPase Subunit V_1B, Encoded by *VMA2*, to Stress Response, Autophagy, and Virulence Is Independent of Environmental pH

Hallie S. Rane,[a] Stella M. Bernardo,[a,b] Summer R. Hayek,[c] Jessica L. Binder,[c] Karlett J. Parra,[c] Samuel A. Lee[a,b]

Section of Infectious Diseases, New Mexico Veterans Healthcare System, Albuquerque, New Mexico, USA[a]; Division of Infectious Diseases[b] and Department of Biochemistry and Molecular Biology,[c] University of New Mexico Health Science Center, Albuquerque, New Mexico, USA

Candida albicans **vacuoles are central to many critical biological processes, including filamentation and *in vivo* virulence. The V-ATPase proton pump is a multisubunit complex responsible for organellar acidification and is essential for vacuolar biogenesis and function. To study the function of the V_1B subunit of *C. albicans* V-ATPase, we constructed a tetracycline-regulatable *VMA2* mutant, tetR-*VMA2*. Inhibition of *VMA2* expression resulted in the inability to grow at alkaline pH and altered resistance to calcium, cold temperature, antifungal drugs, and growth on nonfermentable carbon sources. Furthermore, V-ATPase was unable to fully assemble at the vacuolar membrane and was impaired in proton transport and ATPase-specific activity. *VMA2* repression led to vacuolar alkalinization in addition to abnormal vacuolar morphology and biogenesis. Key virulence-related traits, including filamentation and secretion of degradative enzymes, were markedly inhibited. These results are consistent with previous studies of *C. albicans* V-ATPase; however, differential contributions of the V-ATPase V_o and V_1 subunits to filamentation and secretion are observed. We also make the novel observation that inhibition of *C. albicans* V-ATPase results in increased susceptibility to osmotic stress. Notably, V-ATPase inhibition under conditions of nitrogen starvation results in defects in autophagy. Lastly, we show the first evidence that V-ATPase contributes to virulence in an acidic *in vivo* system by demonstrating that the tetR-*VMA2* mutant is avirulent in a *Caenorhabditis elegans* infection model. This study illustrates the fundamental requirement of V-ATPase for numerous key virulence-related traits in *C. albicans* and demonstrates that the contribution of V-ATPase to virulence is independent of host pH.**

The fungal pathogen *Candida albicans* is the fourth most common cause of hospital-acquired bloodstream infections and is a major cause of catheter-associated infections, sepsis, and device-related infections. It is also an extremely common cause of urinary and mucosal infections. Despite its clinical significance, the diagnosis and treatment of disseminated candidiasis remain limited by an incomplete understanding of its molecular pathogenesis. The fungal vacuole, a degradative organelle roughly equivalent to the mammalian lysosome, plays an important role in numerous biological processes in *C. albicans*, including key aspects of pathogenesis. Previous studies have established that *C. albicans* mutants compromised in vacuolar function are defective in yeast-to-hypha transitioning, a major virulence-related trait, and exhibit reduced virulence *in vivo* (1, 2).

An essential component of vacuolar biogenesis and function is the vacuolar H^+-ATPase (V-ATPase) proton pump, which is a multisubunit complex responsible for the acidification of internal organelles. V-ATPase is located at the vacuolar membrane and throughout the endomembrane system, including prevacuolar compartments and the Golgi complex (1). The acidification of these organelles has several important functions: first, the protons pumped into the compartment by V-ATPase energize multiple secondary transporter systems, such as those involved in metal ion homeostasis, and second, the acidic pH created by V-ATPase is necessary for the activity of degradative enzymes. Accordingly, in both *Saccharomyces cerevisiae* and *C. albicans*, mutations in V-ATPase lead to the Vma^- phenotype, which is characterized by poor growth at alkaline pH as well as defective metal sequestration, glycerol metabolism, and other responses to environmental stress conditions (1, 3–6). V-ATPase mutants are also impaired in vacuolar biogenesis due to defects in both vacuolar membrane fusion and fission (7). In addition to its requirement for intraorganellar pH homeostasis, V-ATPase function has been implicated in cytosolic and extracellular pH homeostasis (1, 8–11), underscoring the far-reaching importance of this pump to overall cellular homeostasis. V-ATPase inhibition also interferes with virulence-related traits in *C. albicans*, including the secretion of degradative enzymes and yeast-to-hypha transitioning (3, 4, 12, 13). Notably, V-ATPase previously has been shown to be important for *in vivo* virulence in *C. albicans* (3, 13); however, the requirement of acidic environmental pH for the growth of V-ATPase mutants complicates the interpretation of these studies due to the growth-limiting alkaline pH in the bloodstream of the murine host.

V-ATPase is composed of two multisubunit domains, V_o and V_1. V_o is embedded in the organellar membrane and is the site of proton transport. V_1 contains the catalytic subunits of the complex responsible for ATP hydrolysis at the cytosolic side of the membrane. The catalytic portion of V-ATPase is a hexamer composed of three copies of V1 subunit A (V_1A) and three copies of V_1

Received 30 May 2014 **Accepted** 12 July 2014
Published ahead of print 18 July 2014
Address correspondence to Samuel A. Lee, SamALee@salud.unm.edu.
Supplemental material for this article may be found at http://dx.doi.org/10.1128/EC.00135-14.

doi:10.1128/EC.00135-14

TABLE 1 List of strains used in this study

Strain	Parent	Relevant genotype	Source
BWP17	SC5314	*ura3*Δ/*ura3*Δ *arg4*Δ/*arg4*Δ *his*Δ/*his1*Δ *VMA2/VMA2*	Wilson et al. (17)
BWP17-*VMA2*Δ/+	BWP17	*ura3*Δ/*ura3*Δ *arg4*Δ/*arg4*Δ *his*Δ/*his1*Δ *VMA2/VMA2*Δ::*dpl200-URA3-dpl200*	This study
THE1	CAI8	*ade2*Δ::*hisG/ade2*Δ::*hisG ura3*Δ::*imm434/ura3*Δ::*imm434 ENO1/eno1*Δ::*ENO1*-tetR-ScHAP4AD-3× HA-*ADE2 VMA2/VMA2*	Nakayama et al. (18)
THE1-CIp10	THE1	*ade2*Δ::*hisG/ade2*Δ::*hisG ura3*Δ::*imm434/ura3*Δ::*imm434 ENO1/eno1*Δ::*ENO1*-tetR-ScHAP4AD-3× HA-*ADE2 RP10/RP10*::*URA3 VMA2/VMA2*	Bernardo et al. (20)
*VMA2*Δ/+	THE1	*ura3*Δ::*imm434/ura3*Δ::*imm434 VMA2/VMA2*Δ::*dpl200-URA3-dpl200 ade2*Δ::*hisG/ade2*Δ::*hisG ura3*Δ::*imm434/ura3*Δ::*imm434 ENO1/eno1*Δ::*ENO1*-tetR-ScHAP4AD-3× HA-*ADE2*	This study
*VMA2*Δ/+ FOA	*VMA2*Δ/+	*ura3*Δ::*imm434/ura3*Δ::*imm434 VMA2/VMA2*Δ::*dpl200 ade2*Δ::*hisG/ade2*Δ::*hisG ura3*Δ::*imm434/ura3*Δ::*imm434 ENO1/eno1*Δ::*ENO1*-tetR-ScHAP4AD-3× HA-*ADE2*	This study
tetR-*VMA2*	*VMA2*Δ/+ FOA	*ura3*Δ::*imm434/ura3*Δ::*imm434 VMA2*Δ::*dpl200*::99t-*VMA2-URA3 ade2*Δ::*hisG/ade2*Δ::*hisG ura3*Δ::*imm434/ura3*Δ::*imm434 ENO1/eno1*Δ::*ENO1*-tetR-ScHAP4AD-3× HA-*ADE2*	This study
tetR-*VMA3*	*VMA3*Δ/+ FOA	*ura3*Δ::*imm434/ura3*Δ::*imm434 VMA3*Δ::*dpl200*::99t-*VMA3-URA3 ade2*Δ::*hisG/ade2*Δ::*hisG ura3*Δ::*imm434/ura3*Δ::*imm434 ENO1/eno1*Δ::*ENO1*-tetR-ScHAP4AD-3× HA-*ADE2*	Rane et al. (4)
T-LAP41-GFP	THE1-CIp10	*ade2*Δ::*hisG/ade2*Δ::*hisG ura3*Δ::*imm434/ura3*Δ::*imm434 ENO1/eno1*Δ::*ENO1*-tetR-ScHAP4AD-3× HA-*ADE2 RP10/RP10*::*URA3 VMA2/VMA2 LAP41/LAP41-GFP-NAT1*	This study
tV2-LAP41-GFP	tetR-*VMA2*	*ura3*Δ::*imm434/ura3*Δ::*imm434 VMA2*Δ::*dpl200*::*99t-VMA2-URA3 ade2*Δ::*hisG/ade2*Δ::*hisG ura3*Δ::*imm434/ura3*Δ::*imm434 ENO1/eno1*Δ::*ENO1*-tetR-ScHAP4AD-3× HA-*ADE2 LAP41/LAP41-GFP-NAT1*	This study

subunit B (V_1B), which alternate in configuration. V_1A is the primary site of ATP hydrolysis, whereas V_1B (encoded by the *VMA2* gene) plays a regulatory role in ATP hydrolysis and contributes to ATP-binding sites (6). Studies of *S. cerevisiae* have shown that disruption of *VMA2* completely inhibits both ATPase activity and proton transport by the V-ATPase (14). We have previously investigated the contribution of several subunits of *C. albicans* V-ATPase to cell biology and virulence-related traits (4, 12). This is the first study analyzing a subunit of the catalytic hexamer in the V_1 domain of V-ATPase in *C. albicans*. We generated a tetracycline-regulatable mutant of *VMA2* in order to establish the contribution of the V_1B subunit of the V-ATPase to pH and stress response, V-ATPase function, and vacuolar morphology. We also analyzed *VMA2* contribution to *C. albicans* virulence-related traits, including filamentation and secretion of degradative enzymes. We next studied the effect of V-ATPase inactivation on autophagy, the recycling of cellular building blocks in response to starvation and stress, by monitoring long-term survival during nitrogen starvation and turnover of the autophagy-related protein Ape1p. Finally, we utilized a *Caenorhabditis elegans* model of infection in the first study of V-ATPase contribution to virulence in an acidic host environment.

MATERIALS AND METHODS

Strains and media. The strains used in this study are listed in Table 1. Standard growth was completed at 30°C in yeast peptone dextrose (YPD; 1% yeast extract, 2% peptone, and 2% glucose) supplemented with 80 μg/ml uridine where required. When needed, doxycycline (DOX) was added to a final concentration of 20 μg/ml. Media were buffered to pH 4.0 to 5.0 using 50 mM succinic acid–50 mM Na_2PO_4 or to pH 7.5 to 8.5 using 50 mM morpholineethanesulfonic acid (MES) hydrate–50 mM morpholinepropanesulfonic acid (MOPS) where required. Unless otherwise specified, agar plates were prepared with 2% agar. For all experiments, cells were grown for 24 h in unbuffered YPD with or without DOX prior to the start of the experiment to ensure the complete turnover of extant Vma2p. Where the pH of the media is not explicitly stated, the media used were not buffered to a specific pH (i.e., unbuffered media). All plates were incubated at 30°C for 48 h unless otherwise stated.

Statistical analyses. Results were analyzed for statistical differences using one-way analysis of variance (ANOVA), followed by Tukey's multiple-comparison test (GraphPad Prism 6). A result was considered significant when $P < 0.05$ compared to all other treatments.

***C. albicans* sequence data.** Sequence data for *C. albicans* were obtained from the Candida Genome Database website at http://www.candidagenome.org.

Attempted disruption of *C. albicans VMA2*. The primers used in this study are listed in Table 2. A BLASTp search of the Candida Genome Database (http://www.candidagenome.org/) revealed a single potential ortholog to *S. cerevisiae* Vma2p (http://www.yeastgenome.org/), *C. albicans orf19.6634*. We first attempted to generate a *VMA2* null mutant in *C. albicans* using a PCR-based gene disruption strategy (15). Primers *VMA2*-5DR and *VMA2*-3DR were used to amplify the *dpl200-URA3-dpl200*-containing plasmid pDDB57 (from A. Mitchell, Carnegie Mellon University). *C. albicans* BWP17 was transformed with the *VMA2*Δ::*dpl200-URA3-dpl200* PCR amplicon using the lithium acetate method. Because *vma* mutants exhibit poor growth at alkaline pH, selective media were buffered to pH 4.0 to 5.0 to facilitate *VMA2* disruption. Genomic DNA was extracted from transformants as described previously (16). The transformants were screened for homologous reintegration via PCR with primers *VMA2*-5Det and *VMA2*-3Det. Disruption of the second allele of *VMA2* was attempted using the *VMA2*-5DR and *VMA2*-3DR primers to amplify the plasmid pRS-ARG4ΔSpeI (from A. Mitchell, Carnegie Mellon University) (17). This *VMA2*Δ::*ARG4* PCR amplicon was used to transform the BWP17-*VMA2*Δ/+ strain via the lithium acetate method using selective media, without arginine, buffered to pH 4.0 or 5.0. The genotype of the transformants was assessed by allele-specific PCR using primers *VMA2*-5Det and *VMA2*-3Det.

Construction of a tetracycline-regulated *VMA2* gene. One *C. albicans VMA2* allele was deleted from the THE1 strain background (18) using PCR-based gene disruption (15) and lithium acetate transformation. Primers *VMA2*-5DR and *VMA2*-3DR (Table 2) were used to amplify plasmid pDDB57. Strain THE1 then was transformed with the resulting PCR amplicon to generate *VMA2*Δ/+ (Table 1). Correct genomic integration of the gene disruption cassette was confirmed via PCR using primers *VMA2*-5Det and *VMA2*-3Det. The *VMA2*Δ/+ strain then was plated to 5-fluoroorotic acid (5-FOA) agar media, and the resultant 5-FOA-resistant colonies were screened via PCR for the *VMA2/VMA2*Δ::*dpl200* genotype using primers *VMA2*-5Det and *VMA2*-3Det. The tetracycline-regulatable system described by Nakayama et al. (18), with modifications described by Bates et al. (19), was used to place the remaining *VMA2* allele under a tetracycline-regulatable promoter. Plasmid p99CAU1 (from H. Nakayama, Suzuka University) was amplified using primers tet*VMA2*-

TABLE 2 Primers used in this study

Primer	Primer sequence (5′–3′)	Source
VMA2–5DR	ATGGAAAAAGAGAGAGTAATTGGCCGTTTCTTATCGTCCTTTTGTTGTACTCTTTTAAATTTTTCA TTTAGTTTTCCCAGTCACGACGTT	This study
VMA2–3DR	ATAGATAATTTTTGTCAGAATTAAAAAAAATGAAAATAATAATGATAATAATAGTAAATAAAACTA ATGATGTGGAATTGTGAGCGGATA	This study
VMA2–5Det	GCAACGAATGGGACATAGTG	This study
VMA2–3Det	GATATGATTGCCAAGGACGG	This study
tetVMA2–5DR	TGATCGAATCTATACCGAGTCTACTACGAATACGGAGGTTACTCAGATCCCAAAAAAATTTGACACTA AAGTAATACGACTCACTATAGGG	This study
tetVMA2–3DR	ATTTTAAACCCTTCTGTGACTGCTTTTTTGTTTAATTCAAACAATTCTTTATCAGAGAGTGACATTATT GCTAGTTTTCTGAGATAAAGCTG	This study
tetVMA2–5Det	GTCATCTGTCGAGCCTGCAG	This study
tetVMA2–3Det	CCATTGACACCACCAACAGT	This study
tetINS-3Det	CTAGTTTTCTGAGATAAAGCTG	Rane et al. (4)
RT-VMA2–5Det	CCACGTTTGGCCTTGACTAC	This study
RT-VMA2–3Det	TCTTCTGTAGACAATGCTTC	This study
LAP41-GFP-5DR	ATTAGGTATTAAATTCTTCTATGGTTTCTTCAAGAATTGGAGAGATGTCTATGATAATTTTGTTGATTT AGGTGGTGGTTCTAAAGGTGAAGAATTATT	This study
LAP41-GFP-3DR	TAAACTAACAAATAACTAATACTTGCAAATCAACTTTTAATGATTCCTTTTCCTGTTGTTCAATGTTCG ACGTTAGTATCGAATCGACAGC	This study
LAP41-GFP-5Det	GCCTTGGCTGAAGAATTGGC	This study
GFP-UP	CACCTTCACCGGAGACAG	Milne et al. (33)

5DR and tet*VMA2*-3DR. The resulting PCR amplicon was inserted upstream of the remaining *VMA2* allele of the *VMA2*Δ/+ 5-FOA strain via lithium acetate transformation. Transformants were screened for the correct insertion of the tetR-*VMA2* allele using primers tet*VMA2*-5Det and tet*VMA2*-3Det (Table 2). Reverse transcription-PCR (RT-PCR) was performed to assay expression of *VMA2* in both the THE1-CIp10 control strain and the tetR-*VMA2* strain after 24 h of growth in YPD with or without DOX. After 24 h of growth in YPD with or without DOX, RNA was extracted from cells using the RiboPure yeast kit (Ambion) according to the manufacturer's protocol, with 1 μl of the RNase inhibitor RNasin (Promega) added after the binding, elution, and DNase I steps to prevent RNA degradation. mRNA then was extracted from total RNA using the PolyATtract mRNA isolation system (Promega) according to the manufacturer's instructions. One μl RNasin was added to each treatment after the final elution step. Finally, RT-PCR was completed with the Access RT-PCR system (Promega) according to the manufacturer's instructions using primers RT-*VMA2*-5Det and RT-*VMA2*-3Det and 5 μg total mRNA as the template. The absence of contaminating DNA was tested in parallel PCR-based reactions.

pH and stress response. The ability of tetR-*VMA2* to respond to various pHs was tested on complete synthetic media (CSM; 0.67% yeast nitrogen base without amino acids [YNB], 0.079% complete synthetic mixture, 2% glucose) agar plates buffered to pH 4.0 to 8.5 with or without DOX. The THE1-CIp10 control strain, a strain from the THE1 background with *URA3* reintegrated into the genome (20), was used as an additional control in this and all subsequent experiments. THE1-CIp10 also was studied with and without DOX to control for the effect of DOX on this and all subsequent experiments. The ability of tetR-*VMA2* to grow on unbuffered media was tested on CSM with or without DOX; unbuffered CSM has a pH of ~6. Cells from overnight cultures were washed and counted as previously described (21); next, 10^8 cells per ml were inoculated in phosphate-buffered saline (PBS). Five 5-fold dilutions then were completed in 96-well plates, and cells were stamped onto agar plates using a multiblot replicator per the manufacturer's instructions (VP 408H; VP Scientific). Plates were incubated at 30°C for 48 h. Growth at pH 4.0 to 8.5 also was tested in liquid media: cells from overnight cultures were diluted to an optical density at 600 nm (OD_{600}) of 0.05 in CSM, pH 4.0 to 8.5, with or without DOX. Cells were grown at 30°C using a Synergy H1 microplate reader (Biotek) with double orbital shaking at fast speed and 2-mm frequency; OD_{600} readings were taken at 15-min intervals.

The ability of tetR-*VMA2* to respond to various stress conditions was tested on agar plates with or without DOX. The calcium stress response was tested on unbuffered YPD plus 200 mM $CaCl_2$. Plates used to test the response of strains to media containing glycerol as the sole carbon source contained unbuffered yeast extract plus peptone (YEP)–2% ethanol–3% glycerol. Plates used to test the response of strains to oxidative stress contained CSM, pH 4.0, with 5 mM H_2O_2; for the oxidative stress assay, plates were incubated at 30°C for 72 h rather than 48 h. The ability of strains to respond to challenge with antifungals was tested on YPD, pH 4.0, with or without DOX with 0.00625 to 0.5 μg/ml amphotericin B (AMB); 0.05 μg/ml caspofungin (CAS); 10 to 20 μg/ml flucytosine (FCT); or 0.6125, 1.25, 2.5, 5, or 10 μg/ml fluconazole (FLU). For fluconazole susceptibility studies, the tetR-*VMA3* strain also was included (4). Temperature sensitivity was assessed by stamping cells onto unbuffered YPD with or without DOX agar plates and incubating at 25°C, 30°C, 37°C, or 42°C for 48 h. CSM, pH 4.0, with or without DOX plates containing either 1 M NaCl, 200 μg/ml Congo red, or 50 μg/ml calcofluor white also were tested. For all plates, cells were stamped onto media using a multiblot replicator as described above.

V-ATPase assembly and activity assays. Starter cultures were grown for 6 to 8 h in YPD, pH 4.0, with or without DOX. Vacuoles were prepared by resetting cells in YPD, pH 4.0, with or without DOX and growing to them to an OD_{600} of 1.0 to 1.5 (18 h). Total growth time in YPD, pH 4, with or without DOX before vacuolar membrane purification was 24 h to 26 h. Ficoll density gradient centrifugation (22) was used to purify vacuolar membranes. For Western blotting, 80 μg of vacuolar protein was separated by SDS-PAGE and transferred to nitrocellulose at 150 mA overnight. The V_1A subunit was visualized with a 1:1,000 dilution of anti-human V_1A rabbit polyclonal antibody, which cross-reacts with *C. albicans* Vma1p (aka V_1A) (23).

In order to quantify ATP hydrolysis, 15 μg purified vacuolar vesicles was used in an enzymatic assay in which the rate of ATP hydrolysis is coupled to the oxidation of NADH, measured as a loss of A_{340} over time (24) in the presence and absence of the V-ATPase inhibitor concanamycin A (12, 25). Proton transport of 30 μg purified vacuolar vesicles was measured via quenching of 1 μM 9-amino-6-chloro-2-methoxyacridine (ACMA) upon the addition of 0.5 mM ATP–1 mM $MgSO_4$ (MgATP) as described previously (25, 26). Fluorescence at excitation and emission wavelengths of 410 nm and 490 nm, respectively, was monitored for 60 s prior to MgATP addition and for 40 s after. Proton transport was calcu-

lated as the change in fluorescence for the first 15 s following MgATP addition. For both assays, 100 nM concanamycin A, a specific V-ATPase inhibitor, was used to assess V-ATPase-specific activity.

Vacuolar acidification assays. Quinacrine staining was performed to visualize acidified vacuoles as described previously (27), with modifications as indicated previously (4). Briefly, cells were grown for 24 h in unbuffered YPD with or without DOX and then reset in fresh unbuffered YPD with or without DOX and grown to early log phase. Cells were stained with 200 μM quinacrine in YPD buffered with 50 mM Na_2PO_4, pH 7.6, for 10 to 15 min. Cells were washed and resuspended in 100 mM HEPES–50 mM Na_2PO_4, pH 7.6–2% glucose before visualization via differential interference contrast (DIC) and fluorescence microscopy. Vacuolar pH was quantified as described previously (12) using 2′-7′-bis-(2-carboxyethyl)-5-(and-6)-carboxyfluorescein-acetoxymethyl ester (BCECF-AM; from Invitrogen).

Vacuolar morphology. For all vacuolar staining, DOX was added to the appropriate treatments upon each medium change. To simultaneously stain vacuoles with FM4-64 [*N*-(3-triethylammoniumpropyl)-4-(6-(4-(diethylamino) phenyl) hexatrienyl) pyridinium dibromide] and CMAC (7-amino-4-chloromethyl coumarin), cells were grown for 24 h in unbuffered YPD with or without DOX. Cells then were reset in fresh unbuffered YPD with or without DOX and grown to early log phase. Cells were resuspended to an OD_{600} of 2 to 4 in unbuffered YPD containing 40 μM FM4-64 and incubated for 15 min at 30°C, reset in fresh unbuffered YPD, and incubated for 45 min at 30°C. Cells were resuspended to an OD_{600} of 0.1 in 10 mM HEPES, 5% glucose, pH 7.4. CMAC was added to a concentration of 100 μM, and cells were incubated at room temperature for 15 min and examined via DIC microscopy and fluorescence microscopy with a Zeiss Axio Imager (Carl Zeiss AG, Germany) using Texas red (FM4-64) and 4′,6-diamidino-2-phenylindole (DAPI) (CMAC) filters.

Filamentation and secretion assays. Filamentation was assessed on solid and in liquid media with or without DOX. Media tested were YPD plus 10% fetal calf serum (FCS), medium 199 supplemented with L-glutamine (M199), Spider medium as previously described (28), and RPMI–L-glutamine. All media were tested unbuffered as well as buffered to pH 4.0. Spider medium was prepared with 1.35% (wt/vol) agar. Three μl cells from overnight cultures were spotted to agar plates and incubated at 37°C for 120 h. Filamentation in liquid media was tested in RPMI–L-glutamine, pH 5.0, with or without DOX. Media were inoculated with cells from overnight cultures to a starting density of 5×10^6 cells per ml, and cells were grown at 37°C, 200 rpm for 2 to 24 h. Cells were visualized via DIC microscopy using a Zeiss EC Plan-NeoFluar 63×/1.25 oil objective (Carl Zeiss AG, Germany) at selected time points.

Aspartyl protease and lipase secretion was assessed on solid media. Extracellular protease secretion was assayed on unbuffered bovine serum albumin (BSA) plates (29), and lipase secretion was assayed on plates containing unbuffered YNB plus 2.5% Tween 80 (30). All plates were prepared with or without DOX. First, cells were grown in YPD with or without DOX for 24 h. Three μl cells then was spotted onto plates. BSA plates were incubated at 30°C for 48 h, and Tween 80 plates were incubated at 37°C for 120 h. For aspartyl protease secretion, the relative halo size was calculated using the software program TotalLab 100. First, THE1-CIp10 and tetR-*VMA2* were grown in YPD with or without DOX for 24 h, and then 3 μl cells from each treatment was spotted onto six BSA plates and onto six BSA-plus-DOX plates. Plates were grown at 30°C for 48 h and scanned. For each colony spot, the areas, in pixels of the colony alone and of the halo and colony combined, were quantified using TotalLab 100. The relative area of the halo was calculated as the area of the halo and colony divided by the area of the colony alone; a relative halo size of 1 would indicate a lack of detectable halo. Relative halo size is given as the averages ± standard deviations from 6 replicates. One-way ANOVA was used to compare the relative halo area for each treatment.

Long-term survival during nitrogen starvation. In order to assess the ability of tetR-*VMA2* to survive long-time nitrogen starvation, we analyzed tetR-*VMA2* resistance to nitrogen starvation using a previously described assay (31). Strains THE1-CIp10 and tetR-*VMA2* first were grown for 24 h in unbuffered YPD ± DOX, and then 10^8 cells per treatment were transferred to a microcentrifuge tube and washed twice in 1 ml nitrogen starvation media (i.e., SD − N; 0.17% YNB without ammonium sulfate or amino acids plus 2% glucose) before resuspending in 1 ml SD − N. One hundred μl of this cell suspension was added to 4.9 ml SD − N with or without DOX for a final cell concentration of 2×10^6 cells per ml. At 24-h intervals, fresh DOX to a concentration of 20 μg/ml was added to appropriate treatments. Dilutions (1:1,000) were completed at selected time points. One hundred μl of the resulting dilution was plated to YPD in triplicate for CFU counts. On days 0, 10, 20, and 30 of the experiment, the pH of the media was tested by transferring 100 μl SD − N from each treatment to pH test strips (Sigma-Aldrich).

In order to further study the contribution of *VMA2* to autophagy, we utilized the commonly used autophagy marker aminopeptidase I (Ape1), encoded by the *C. albicans LAP41* gene (31, 32). Ape1p was C-terminally tagged with green fluorescent protein (GFP) in the THE1-CIp10 and tetR-*VMA2* backgrounds to generate strains T-LAP41-GFP and tV2-LAP41-GFP (Table 1). First, primers LAP41-GFP-5DR and LAP41-GFP-3DR (Table 2) were used to amplify the GFP-*NAT1* cassette from plasmid pGFP-NAT1 (from S. Bates, University of Exeter) (33); these primers use 70 nucleotides of *LAP41* homologous targeting sequences as previously described (31), combined with sequences for amplification of the GFP-*NAT1* cassette (33). Strains THE1-CIp10 and tetR-*VMA2* were transformed with the resulting PCR amplicon as previously described (33), and transformants were selected for on Sabouraud-dextrose agar (BD, Franklin Lakes, NJ) containing 200 μg/ml nourseothricin (Gold Biotechnology, St. Louis, MO). Primers LAP41-GFP-5Det and GFP-UP (Table 2) were used to screen for correct integration of the *LAP41*-GFP allele. For visualization of Ape1-GFP, strains T-LAP41-GFP and tV2-LAP41-GFP were grown for 24 h in unbuffered YPD with or without DOX prior to the start of the experiment. Cells then were washed twice in PBS, resuspended to an OD_{600} of 0.2 in fresh SD − N with or without DOX, and grown at 30°C for 1 h at 200 rpm. FM4-64 was added to a concentration of 40 μM. Cells were grown at 30°C for 15 min at 200 rpm, spun down, and resuspended in fresh SD − N with or without DOX media to remove excess FM4-64 stain. Cells were grown at 30°C for 20 days at 200 rpm, with fresh DOX added to appropriate treatments to a concentration of 20 μg/ml at 24-h intervals. After 2, 4, 6, 24, 48, 120, and 240 h in nitrogen starvation media, cells were visualized with a Zeiss Axio Imager and AxioVision 4.7 software (Carl Zeiss AG, Germany). Ape1-GFP fluorescence images were acquired using a GFP cube (400-ms exposure time), and FM4-64 fluorescence images were acquired using a Texas red cube (100-ms exposure time).

***C. elegans* infection assays.** *C. elegans* solid medium killing assays were performed as described previously (34), with some important modifications. First, all infection assays were completed at 30°C rather than 25°C due to the cold sensitivity of the tetR-*VMA2* strain upon DOX repression (see Fig. 2A). Further, previous studies have utilized either *C. elegans glp-4;sek-1* nematodes rather than wild-type nematodes (35) or treatment with 5-fluoro-2′-deoxyuridine (34) to avoid the complicating presence of eggs and larvae during the infection assay. However, because our experiments were conducted at 30°C, a temperature at which *C. elegans* reproduction, but not viability, is completely inhibited (36), we were able to use the *C. elegans* wild-type strain, N2. To ensure that exposure to chronic heat stress or doxycycline was not the primary cause of worm mortality, we utilized negative controls in which nematodes were exposed to heat-killed *C. albicans* cells, which have previously been shown to be avirulent (34). Negative controls were maintained at an elevated temperature (30°C) with or without DOX for the duration of the experiment.

Routine maintenance of *C. elegans* N2 nematodes was performed at 15°C as described previously (37). Prior to the start of the infection assay, nematodes were synchronized to the same life stage via egg axenization as described previously (37) and then incubated on plates of nematode growth media (NGM; 3 g NaCl, 2.5 g peptone, 17 g agar supplemented

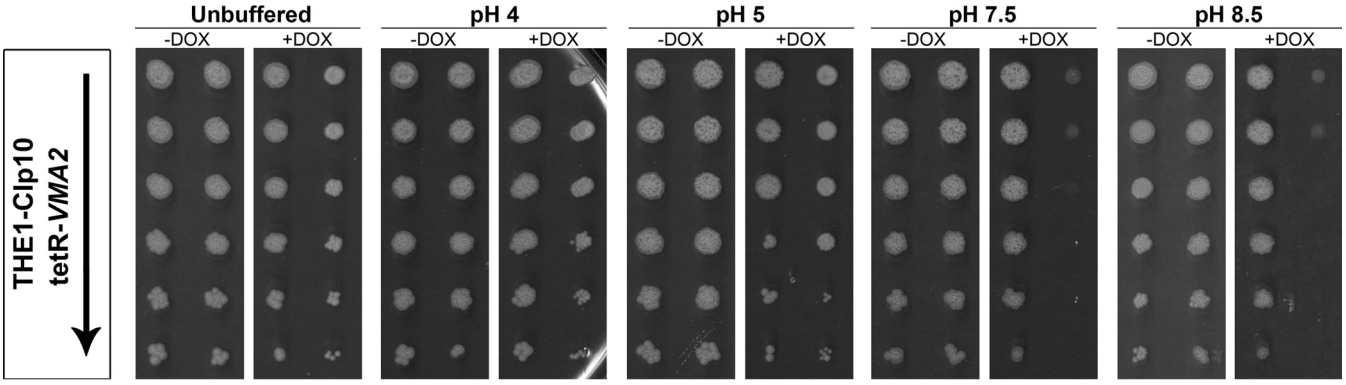

FIG 1 tetR-*VMA2* exhibits the Vma$^-$ phenotype. Serial dilutions of cells grown in YPD with or without DOX for 24 h were spotted onto CSM agar media with or without DOX and incubated for 48 h at 30°C. Strains are indicated on the left, with an arrow signifying decreasing cell densities (1×10^8, 2×10^7, 4×10^6, 8×10^5, 1.6×10^5, and 3.2×10^4 cells per ml) of the strains spotted onto each plate. From left to right, growth was tested on unbuffered CSM, CSM buffered to pH 4 and 5 with 50 mM succinic acid–50 mM Na_2PO_4, and CSM buffered to pH 7.5 and 8.5 with 50 mM MES hydrate–50 mM MOPS.

with 1 mM $CaCl_2$, 5 μg/ml cholesterol, 1 mM $MgSO_4$, and 25 mM KPO_4 buffer, as described previously [37]) plus *E. coli* OP50 at 15°C until worms reached the L4 stage. For the infection assay, *C. albicans* THE1-CIp10 and tetR-*VMA2* cells first were grown in YPD with or without DOX for 24 h to ensure complete repression of *VMA2*. Plates of YPD (pH 4) with or without DOX then were seeded with a lawn of 50 μl THE1-CIp10 or tetR-*VMA2* cells that had been pretreated with DOX or left untreated. For negative controls, lawns of heat-killed cells were prepared on agar plates of YPD, pH 4, with or without DOX as described previously (34). The plates were incubated at 30°C for approximately 16 h. Synchronized L4 worms were washed from plates with sterile M9 buffer and collected via centrifugation for 1 min at 6,000 rpm. Approximately 500 worms were transferred to the center of the *C. albicans* lawns. For negative controls, approximately 500 worms were transferred to the center of lawns containing heat-killed yeast. All plates were incubated at 30°C for 4 h. After the 4-h infection, *C. elegans* nematodes were washed from the plate, taking care not to disturb the yeast lawn, and were washed in sterile M9 buffer and collected via centrifugation for 1 min at 6,000 rpm. Worms in M9 buffer were transferred to the center of unseeded NGM with or without DOX plates and incubated at 30°C to allow the M9 buffer to dry. Once dry, 80 to 100 nematodes per treatment were pick transferred using a platinum wire to a plate of fresh, unseeded NGM with or without DOX. Worms were monitored twice daily for survival, and surviving nematodes were transferred via platinum wire pick to plates of fresh, unseeded NGM with or without DOX once daily. Transfer to fresh NGM with or without DOX served two purposes: first, to avoid DOX oxidation due to light exposure, and second, to minimize the growth of *C. albicans* originating from either the original infection plate or from the worms' intestines. *C. albicans* lawns are opaque under a dissecting microscope, making monitoring worm survival difficult. Nematodes on heat-killed yeast lawns were not transferred daily. Worms were scored as dead if they did not respond to stimulation with a platinum wire pick. GraphPad Prism 6.0 was used to plot survival curves, calculate differences in survival (log-rank and Wilcoxon tests) via the Kaplan-Meier method, and calculate the LT_{50} (defined as the time for half of the worms to die). Dead worms were visualized via light microscopy at selected time points.

RESULTS

***VMA2* is repressed by DOX in the tetR-*VMA2* strain.** Our initial attempt to disrupt *C. albicans VMA2* by generating a *vma2*Δ homozygous null mutant on acidic media was unsuccessful; after screening over 150 transformants from three separate lineages of heterozygous null mutants, a homozygous null mutant was not recovered. These results are consistent with previous attempts to disrupt V-ATPase genes in *C. albicans* (4). Therefore, we constructed the strain tetR-*VMA2*, a tetracycline-regulatable *VMA2* mutant in which the *VMA2* gene is repressed upon the addition of DOX (18). A strain from the THE1 background with *URA3* reintegrated into the genome, THE1-CIp10, was used as an additional wild-type control (20). In order to confirm repression of *VMA2* with DOX, we utilized RT-PCR to analyze *VMA2* expression in the tetR-*VMA2* strain (see Fig. S1 in the supplemental material). We have previously shown that, in a tetracycline-regulatable *VMA3* mutant, the *VMA3* transcript remained present for up to 18 h after treatment with DOX but disappeared completely after 24 h (4). Therefore, we pretreated THE1-CIp10 cells and tetR-*VMA2* cells for 24 h in YPD with or without DOX before extracting mRNA for use in our transcriptional analysis. Treatment with DOX did not affect the *VMA2* transcript level in the THE1-CIp10 control (see Fig. S1 in the supplemental material). Elevated levels of *VMA2* transcript were detected in tetR-*VMA2* without DOX compared to the levels of *VMA2* transcript in the controls of THE1-CIp10 with or without DOX; this is consistent with higher levels of expression observed in other genes when placed under the tetracycline-regulatable (tetR) promoter (18). After 24 h of treatment with DOX, no *VMA2* transcript was detected in the tetR-*VMA2* strain (see Fig. S1). Thus, for all subsequent experiments, cells from the THE1-CIp10 and tetR-*VMA2* strains were grown for 24 h in YPD with or without DOX to ensure complete repression of the *VMA2* gene.

tetR-*VMA2* exhibits the Vma$^-$ phenotype upon repression of *VMA2*. V-ATPase inhibition is lethal under certain conditions, including alkaline pH, the presence of heavy metals, and nonfermentable carbon sources; these traits are referred to collectively as the Vma$^-$ phenotype (6). To test whether inhibition of *C. albicans VMA2* results in the Vma$^-$ phenotype, we tested the growth of tetR-*VMA2* cells that had been pretreated with DOX on CSM with or without DOX plates that were either unbuffered or buffered to pH 4 to 8.5. Wild-type *C. albicans* cells grew as well on media buffered to pH 4 to 8.5 as on unbuffered media (Fig. 1). tetR-*VMA2* cells grew comparably to wild-type cells without DOX under all conditions tested but grew poorly on alkaline media with DOX (Fig. 1, pH 7.5 and pH 8.5). It is worth noting that although tetR-*VMA2* cells with DOX grow as well as the wild type on un-

buffered media and media buffered to pH 4 or 5, wild-type cells but not tetR-*VMA2* cells with DOX treatment form hyphae under these conditions, as evidenced by a wrinkly rather than smooth appearance caused by filamentous structures radiating from the colony. Therefore, inhibition of *C. albicans VMA2* expression leads to the Vma$^-$ growth phenotype, indicating that V-ATPase function is significantly impaired. The Vma$^-$ phenotype also was observed in liquid cultures of CSM, pH 4.0 to 8.5 (data not shown).

Repression of *VMA2* inhibits various stress responses in *C. albicans*. V-ATPase is involved in multiple stress responses, partially due to the formation of a membrane potential across the vacuolar membrane that drives secondary transporters, resulting in the sequestration of harmful compounds inside the vacuole. To test *VMA2* contribution to stress response in *C. albicans*, we grew tetR-*VMA2* cells under various stress conditions. First, we tested the temperature response by plating DOX-pretreated tetR-*VMA2* cells on YPD with or without DOX plates and incubating them at 25°C, 30°C, and 37°C. The THE1-CIp10 control strain with or without DOX and the tetR-*VMA2* strain without DOX grew robustly at all three temperatures (Fig. 2A). These strains began to filament at 30°C and formed filamentous structures at 37°C; high temperature is one of many filamentation-induction signals in *C. albicans* (38). Upon repression of *VMA2* with DOX, the tetR-*VMA2* strain grew poorly at 25°C compared to controls, indicating poor tolerance of low temperature (Fig. 2A). We also observed the absence of filamentous structures in tetR-*VMA2* plus DOX at both 30°C and 37°C (Fig. 2A).

V-ATPase function also is necessary for stress response under conditions such as growth on media containing high concentrations of calcium chloride and media containing glycerol as the sole carbon source (6). Therefore, we tested the response of the tetR-*VMA2* strain to these stress conditions. Compared to the controls (THE1-CIp10 with or without DOX), tetR-*VMA2* grew poorly upon repression of *VMA2* on CSM plates plus 200 mM $CaCl_2$ and on YEP plates plus 2% ethanol plus 6% glycerol (Fig. 2B). The tetR-*VMA2* strain grew at wild-type levels on plates containing high concentrations of sodium chloride and on plates containing high concentrations of the cell wall stressors Congo red and calcofluor white (data not shown); these growth conditions have not been associated with the Vma$^-$ phenotype.

V-ATPase also has been shown to be important for the response to hypoxia in *S. cerevisiae*; *S. cerevisiae* V-ATPase mutants are hypersensitive to oxidative stress, and a *S. cerevisiae vma2*Δ mutant exhibits high levels of reactive oxygen species and oxidative protein damage even in the absence of an oxidant (39). Oxidative stress response is of particular interest in fungal pathogenesis, as it has been shown to be important for host colonization in *C. albicans* (40–42). Therefore, we tested tetR-*VMA2* response to oxidative stress by growing strains on plates of CSM, pH 4, containing 5 mM H_2O_2. In the presence of 5 mM H_2O_2, repression of *VMA2* led to a dramatic decrease in cell viability (Fig. 2B).

V-ATPase has been hypothesized to contribute to the activity of two classes of antifungal drugs: azoles, such as fluconazole, and polyenes, such as amphotericin B (43, 44). We asked whether the tetR-*VMA2* strain was susceptible to four classes of antifungal drugs: echinocandins, polyenes, the antimetabolite flucytosine, and azoles. We tested tetR-*VMA2* growth in the presence of sublethal concentrations of a polyene-class drug, amphotericin B; an echinocandin, caspofungin; and an antimetabolite, flucytosine.

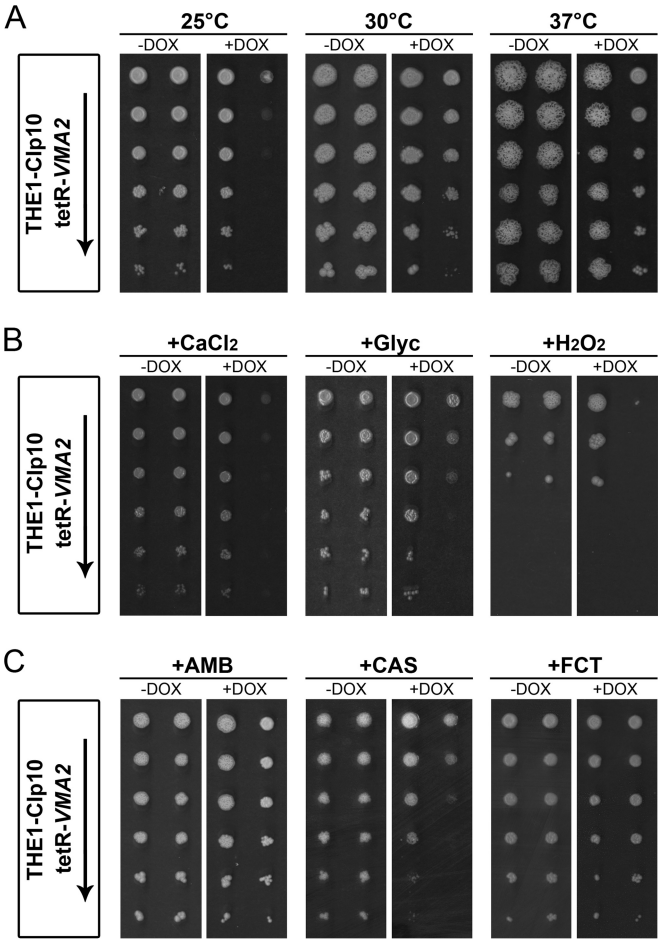

FIG 2 tetR-*VMA2* has decreased tolerance for various stress conditions. Serial dilutions of cells grown in YPD with or without DOX for 24 h were spotted onto different agar media with or without DOX and incubated for 48 h at 30°C. For the oxidative stress assay, plates of CSM, pH 4, plus 5 mM H_2O_2 were incubated at 30°C for 72 h rather than 48 h. Strains are indicated on the left, with an arrow signifying decreasing cell densities (1×10^8, 2×10^7, 4×10^6, 8×10^5, 1.6×10^5, and 3.2×10^4 cells per ml) of the strains spotted onto each plate. (A) tetR-*VMA2* grows poorly on unbuffered YPD plus DOX at 25°C. From left to right, growth was tested on unbuffered YPD agar with or without DOX incubated at 25°C, 30°C, and 37°C. (B) Repression of *VMA2* leads to reduced tolerance to calcium, nonfermentable carbon sources, and oxidative stress. From left to right, tetR-*VMA2* growth was tested on unbuffered CSM with or without DOX with 200 mM $CaCl_2$ added, on unbuffered yeast extract plus peptone (YEP) plus 2% ethanol plus 6% glycerol with or without DOX, and on CSM, pH 4.0, with or without DOX with 5 mM H_2O_2 added. (C) tetR-*VMA2* has increased susceptibility to caspofungin. From left to right, growth was tested on CSM, pH 4.0, with or without DOX with 0.00625 μg/ml amphotericin B, 0.05 μg/ml caspofungin, and 10 μg/ml flucytosine.

THE1-CIp10 and tetR-*VMA2* cells were plated on CSM, pH 4, with or without DOX with 0.00625 to 0.5 μg/ml amphotericin B, 0.05 μg/ml caspofungin, or 10 to 20 μg/ml flucytosine. *VMA2* repression decreased the resistance of the tetR-*VMA2* strain to caspofungin (Fig. 2C) in accordance with previous results (4). In the presence of either 0.00625 μg/ml amphotericin B or 10 μg/ml flucytosine, tetR-*VMA2* cells treated with DOX grew at levels comparable to those of the wild type (Fig. 2C). No difference in growth in the presence of higher levels of either amphotericin B or flucytosine was observed (data not shown).

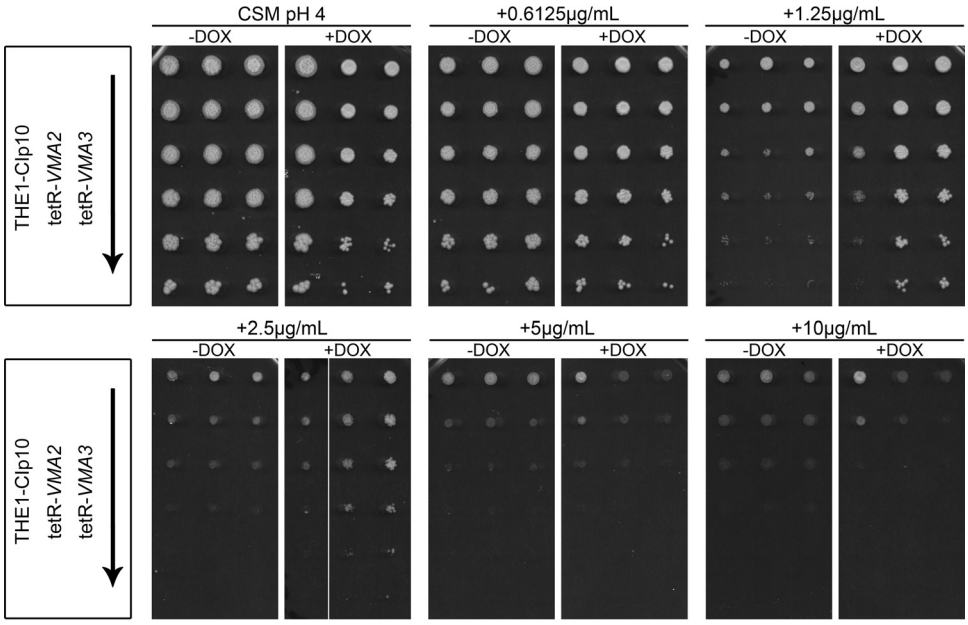

FIG 3 tetR-*VMA2* and tetR-*VMA3* have decreased susceptibility to fluconazole. Serial dilutions of THE1-CIp10, tetR-*VMA2*, and tetR-*VMA3* cells grown in YPD with or without DOX for 24 h were spotted onto CSM agar media with or without DOX and incubated for 48 h at 30°C. Strains are indicated on the left, with an arrow signifying decreasing cell densities (1×10^8, 2×10^7, 4×10^6, 8×10^5, 1.6×10^5, and 3.2×10^4 cells per ml) of the strains spotted onto each plate. Conditions tested in the top row are, from left to right, CSM, pH 4.0, as a control, CSM, pH 4, plus 0.6125 μg/ml fluconazole (FLU), and CSM, pH 4, plus 1.25 μg/ml FLU. The bottom row shows, from left to right, CSM, pH 4, plus 2.5 μg/ml FLU; CSM, pH 4, plus 5 μg/ml FLU; and CSM, pH 4, plus 10 μg/ml FLU.

Because fluconazole activity has been linked previously to V-ATPase function (43), we studied tetR-*VMA2* response to fluconazole in further detail. We tested various concentrations of fluconazole (0.6125 to 10 μg/ml) in tetR-*VMA2* and the previously studied V-ATPase V_oc-deficient strain tetR-*VMA3* (4). Interestingly, repression of *VMA2* and *VMA3* in tetR-*VMA2* and tetR-*VMA3* cells, respectively, increased *C. albicans* growth on plates containing fluconazole at concentrations ranging from 1.25 to 2.5 μg/ml (Fig. 3). At higher concentrations, the growth of the tetR-*VMA2* and tetR-*VMA3* strains was suppressed to levels comparable to those of wild-type cells regardless of the absence or presence of DOX (Fig. 3). Therefore, repression of either V-ATPase V_o or V_1 components results in increased resistance to fluconazole.

Repression of *VMA2* inhibits V-ATPase assembly and activity and leads to vacuolar alkalinization. To establish the effect of *VMA2* suppression on V-ATPase assembly and catalytic activity, we purified vacuolar membrane vesicles from cells grown in YPD, pH 4.0, with or without DOX for 24 h by density gradient centrifugation. Western blots using an antibody against the catalytic subunit A of V_1 (V_1A or Vma1p) did not detect the V_1A subunit in vacuolar membrane fractions under repressing conditions (Fig. 4A), indicating that V-ATPase complexes are not fully assembled. As expected, deletion of the V_1B subunit in *C. albicans* prevented assembly of the V_1 domain at the membrane.

The V_1 domain contains the three catalytic sites where ATP binds and is hydrolyzed, whereas the V_o domain contains the sites of proton binding and transport. Thus, structural coupling of V_1 and V_o is necessary for V-ATPase function (1). The assembly defect of the V-ATPase complex upon depletion of Vma2p is predicted to significantly reduce ATP hydrolysis and proton transport. Therefore, we measured both ATP hydrolysis and proton transport in purified vacuolar membrane vesicles. ATP hydrolysis was measured spectrophotometrically using a coupled enzymatic assay (24). Upon repression of *VMA2*, concanamycin A-sensitive ATP hydrolysis decreased by 91.5% (Fig. 4B). Proton transport was measured fluorometrically using ACMA (25, 26). Repression of *VMA2* with DOX in tetR-*VMA2* completely abrogated proton transport (101.2%) (Fig. 4C). These results are in agreement with the alkalinization of the vacuole in tetR-*VMA2* plus DOX and show that *C. albicans VMA2* is required for both ATPase hydrolysis and proton transport by the V-ATPase.

To confirm that *VMA2* repression inhibits vacuolar acidification by V-ATPase, THE1-CIp10 and tetR-*VMA2* cells with or without DOX were stained with quinacrine, a basic dye that accumulates in the vacuole and fluoresces in acidic environments. The THE1-CIp10 control with or without DOX and the tetR-*VMA2* strain grown without DOX exhibited wild-type quinacrine staining of an acidic vacuole (Fig. 4D). In contrast, the tetR-*VMA2* strain grown in the presence of DOX lacked quinacrine staining of the vacuoles, indicating an alkalinized vacuole (Fig. 4D). In order to quantitatively confirm this phenotype, cells were stained with BCECF, a pH-sensitive fluorophore that accumulates in the vacuole. By comparing the fluorescence profile of BCECF-treated cells to that of a calibration curve, vacuolar pH can be quantitatively determined (10, 25, 45). We previously studied vacuolar pH in the THE1-CIp10 strain both with and without DOX; the vacuolar pH was approximately 6.25 under both conditions (4). The vacuolar pH in the tetR-*VMA2* strain without DOX was 6.099 ± 0.1475. Repression of *VMA2* with DOX resulted in an increase in pH to 6.924 ± 0.05126, indicating vacuolar alkalinization.

Repression of *VMA2* leads to abnormal vacuolar morphology. V-ATPase has been implicated in vacuolar biogenesis, a phenotype attributable to the role of V-ATPase in vacuolar membrane

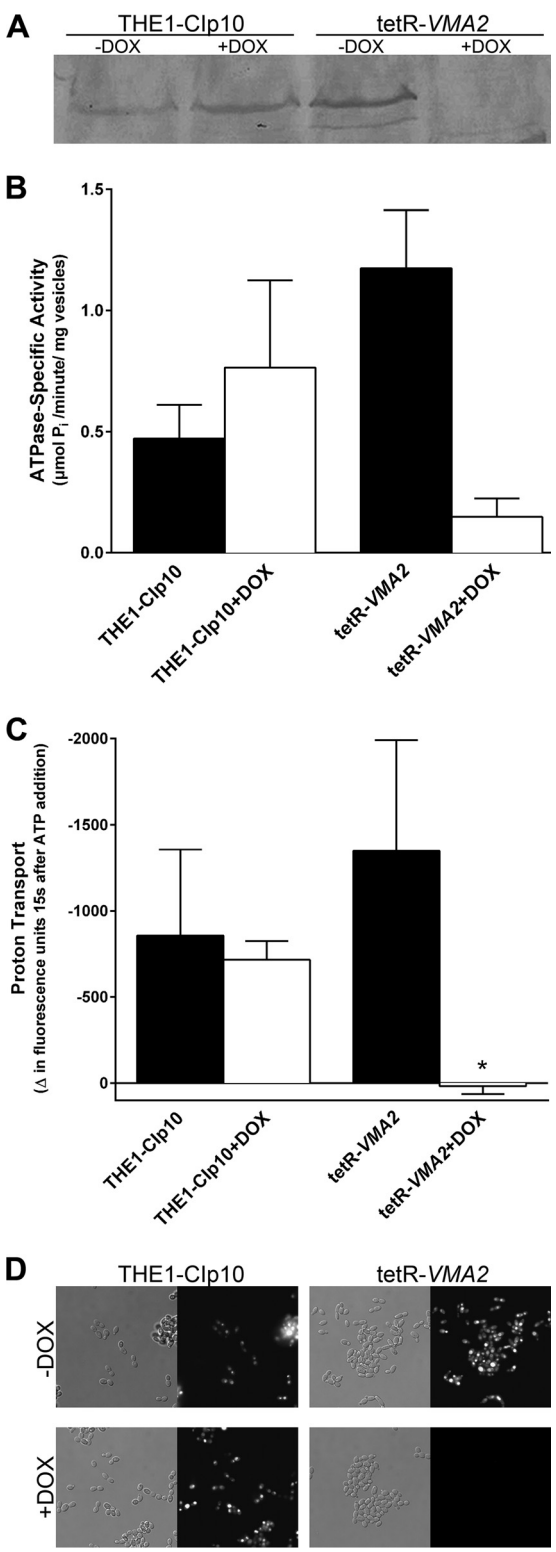

FIG 4 V-ATPase assembly and activity assays. (A) The V-ATPase is not fully assembled at the vacuolar membrane upon *VMA2* repression. Western blots of vacuolar membrane fractions isolated from THE1-CIp10 and tetR-*VMA2* with or without DOX were probed with anti-human-V_1A rabbit polyclonal antibody. (B) DOX repression of *VMA2* leads to decreased ATPase activity. V-ATPase-specific activity (concanamycin A-sensitive ATP hydrolysis) was measured in isolated vacuolar membrane vesicles from THE1-CIp10 and tetR-*VMA2* cells with or without DOX in an enzymatic assay. (C) Proton transport is absent upon repression of *VMA2*. Proton transport in isolated vacuolar membrane vesicles isolated from THE1-CIp10 and tetR-*VMA2* with or without DOX cells was measured using ACMA. Fluorescence was monitored for 60 s prior to MgATP addition and for 40 s afterwards. Proton transport was calculated as the change in fluorescence for the first 15 s following MgATP addition. The asterisk denotes statistical significance compared to all other treatments ($P < 0.05$). (D) DOX-treated tetR-*VMA2* vacuoles do not stain with quinacrine *in vivo*. Cells were grown for 24 h in unbuffered YPD with or without DOX before staining with 200 mM quinacrine and observation via DIC and fluorescence microscopy.

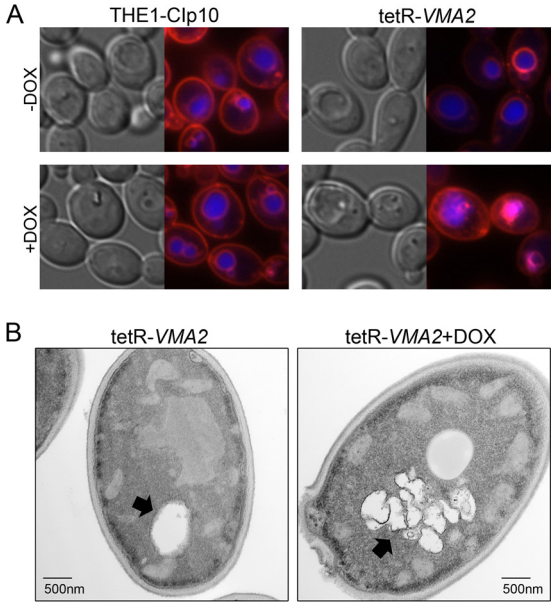

FIG 5 Vacuolar morphology. (A) FM4-64 and CMAC dual staining of vacuoles. To simultaneously stain vacuoles with FM4-64 and CMAC, cells were grown for 24 h in unbuffered YPD with or without DOX. Cells then were reset in fresh unbuffered YPD with or without DOX and grown to early log phase before costaining with FM4-64 and CMAC. Cells were examined via DIC and fluorescence microscopy using Texas red (FM4-64) and DAPI (CMAC) filters. (B) Thin-section electron microscopy showing the tetR-*VMA2* strain after growth in unbuffered YPD with or without DOX for 24 h. In each panel, the black arrow is pointing to the vacuole.

fission and fusion (7, 46, 47). Therefore, we assessed the effect of *VMA2* suppression on vacuolar morphology by simultaneously utilizing two vacuolar stains, FM4-64 and CMAC. FM4-64 is a vital dye that is endocytosed to the vacuole, where it stains the vacuolar membrane (48). CMAC passively accumulates in the vacuolar lumen and stains the vacuolar lumen under both acidic and alkaline conditions. THE1-CIp10 cells both with and without DOX showed well-defined vacuoles, with the FM4-64 membrane stain and the CMAC lumenal stain remaining distinct from one another (Fig. 5A). Without DOX, the tetR-*VMA2* cells showed vacuolar morphology indistinguishable from that of the wild type (Fig. 5A). However, upon DOX repression of *VMA2*, the FM4-64 membrane and the CMAC lumenal stain showed considerable overlap, with membranous structures on the interior of the vacuole revealed by FM4-64 staining (Fig. 5A). We additionally analyzed vacuolar morphology in tetR-*VMA2* cells with or without DOX using thin-section electron microscopy. Vacuolar morphology in the THE1-CIp10 strain, both with and without DOX, has been analyzed previously (20). The tetR-*VMA2* cells without DOX

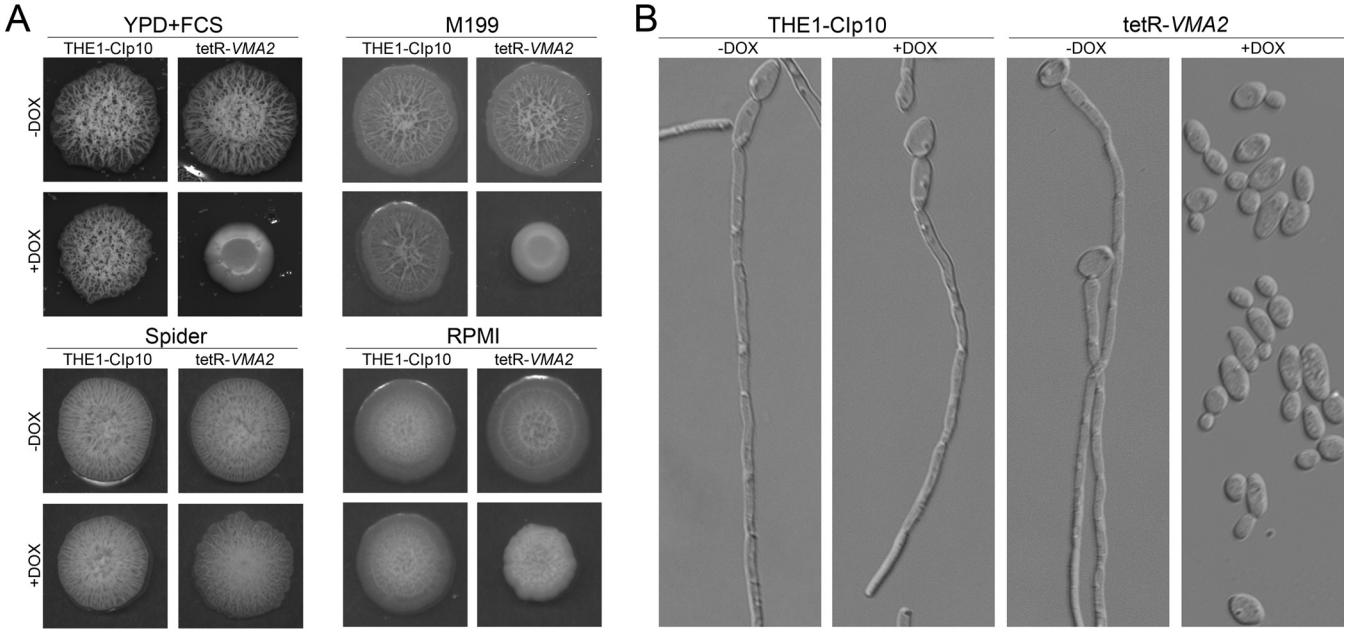

FIG 6 Filamentation on solid and in liquid media. (A) Filamentation on hypha-inducing agar plates. Cells were grown in unbuffered YPD with or without DOX for 24 h. Three μl cells was spotted onto agar plates containing YPD plus FCS, M199, Spider, or RPMI with or without DOX. All plates were buffered to pH 4 with 50 mM succinic acid–50 mM Na_2HPO_4. Plates were incubated at 37°C for 5 days. (B) Filamentation in liquid RPMI. Cells were grown in unbuffered YPD with or without DOX for 24 h, and then 5×10^6 cells/ml were added to RPMI, pH 5.0, with or without DOX and grown for 24 h at 37°C. Filaments were visualized via DIC microscopy. A representative image from each treatment is shown.

addition displayed wild-type vacuolar morphology, as indicated by the presence of a single, large vacuole (Fig. 5B). However, when treated with DOX for 24 h, the tetR-*VMA2* cells had enlarged vacuoles with excessive internal membranous structures (Fig. 5B). This phenotype is consistent with a defect in vacuolar membrane fission (7).

***VMA2* contributes to *C. albicans* virulence-related traits.** Vacuolar function has been implicated in several key traits of *C. albicans* pathogenesis, including the ability to switch between hyphal and yeast forms of growth. Therefore, we assessed the ability of the tetR-*VMA2* strain to form hyphae *in vitro*. On solid media (YPD plus FCS, M199, and Spider media), the tetR-*VMA2* strain exhibited dramatically reduced filamentation (data not shown). However, because the tetR-*VMA2* strain has reduced growth at alkaline pH, these results were difficult to interpret. Therefore, we assessed *in vitro* filamentation by tetR-*VMA2* on solid and in liquid media buffered to pH 4.0 or pH 5.0. The THE1-CIp10 control strain readily formed hyphae even under acidic conditions (4). On all types of media tested, the tetR-*VMA2* strain grown under nonrepressing conditions produced hyphae at levels comparable to that of the THE1-CIp10 control strain. In contrast, under repressing conditions, the tetR-*VMA2* strain did not produce hyphae on serum or M199 plates and produced less robust hyphal structures on RPMI plates (Fig. 6A). Interestingly, on Spider media, which causes induction of filamentation in response to nutrient-poor conditions (49), the tetR-*VMA2* strain produced hyphae to the same degree as the THE1-CIp10 control even upon repression of *VMA2*. Lastly, we tested *in vitro* filamentation in liquid RPMI, pH 5. Under repressing conditions, tetR-*VMA2* cells were present predominantly in the yeast form even after 24 h of incubation in liquid RPMI, pH 5, at 37°C (Fig. 6B).

The secretion of degradative enzymes also is involved in *C. albicans* pathogenesis by assisting in the invasion of host tissues (50, 51). We assayed *in vitro* secretion of lipases and aspartyl proteases on YNB-Tween 80 and BSA media, respectively (Fig. 7). Wild-type *C. albicans* cells spotted onto media containing lipids, such as YNB-Tween 80 media, secrete lipases resulting in a halo of precipitation around the colony. Under repressing conditions, tetR-*VMA2* exhibited decreased lipolytic activity on YNB-Tween 80 agar (Fig. 7). *C. albicans* cells spotted on media containing BSA as the sole nitrogen source secrete secreted aspartyl proteases (SAPs) that digest the BSA, resulting in a halo of proteolysis around the colony (29). The THE1-CIp10 control strain and the

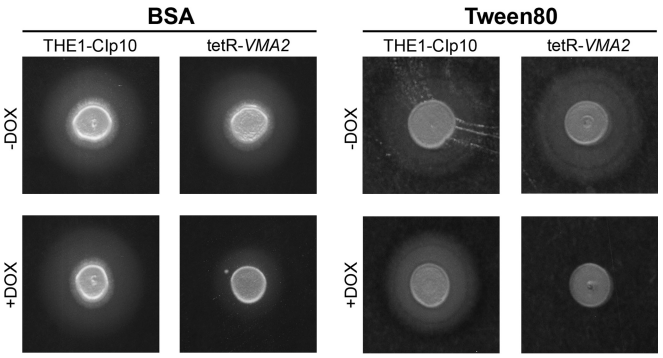

FIG 7 SAP and lipase secretion on Tween 80 and BSA agar. Cells were grown in unbuffered YPD with or without DOX for 24 h, and then 3 μl of cells was spotted onto unbuffered Tween 80 agar plates and unbuffered bovine serum albumin (BSA) agar plates with or without DOX. Unbuffered plates of Tween 80 with or without DOX were incubated at 37°C for 5 days, and plates of unbuffered BSA with or without DOX were incubated at 30°C for 48 h. The relative amount of lipolytic and proteolytic degradation is indicated by the halo surrounding the fungal colony.

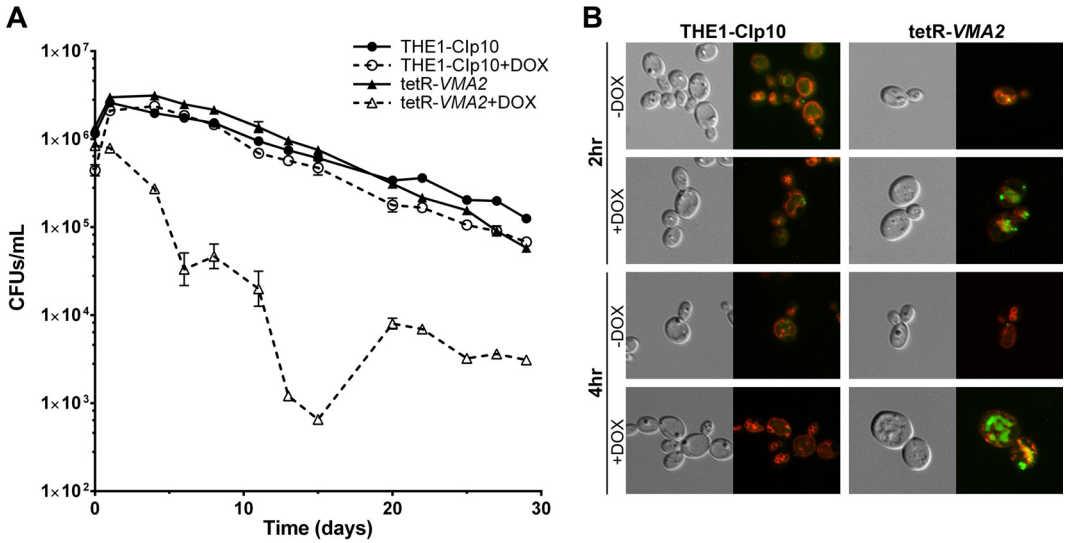

FIG 8 tetR-*VMA2* contribution to autophagy. (A) Resistance to nitrogen starvation in tetR-*VMA2*. Long-term survival of autophagy was determined by CFU counts. Cells were grown for 24 h in unbuffered YPD with or without DOX. Cells then were reset in nitrogen starvation media (SD − N) and grown for 30 days, with samples taken at select time points for CFU counts. (B) Ape1-GFP turnover in tetR-*VMA2*. T-LAP41-GFP and tV2-LAP41-GFP cells were transferred to liquid nitrogen starvation media (SD − N with or without DOX) after 24 h of growth in rich media (YPD with or without DOX). After 115 min of growth at 30°C, cells were coincubated with FM4-64 for 15 min, resuspended in fresh nitrogen starvation media, and grown at 30°C. Cells were visualized via DIC and fluorescence microscopy to detect Ape1-GFP and FM4-64 fluorescence 2 h and 4 h after transfer to nitrogen starvation media.

tetR-*VMA2* strain exhibited normal proteolytic activity under derepressing conditions. DOX repression partially inhibited extracellular proteolytic activity in the tetR-*VMA2* strain (Fig. 7). Because the defect in protease secretion was partial, we quantified the size of the proteolytic halo relative to the size of the colony. For reference, a relative halo size of 1 indicates a lack of detectable halo. For the THE1-CIp10 strain with and without DOX, the relative sizes of the proteolytic halos were 3.605 ± 0.4848 and 3.655 ± 0.8016, respectively. For the tetR-*VMA2* strain without DOX, the relative size of the proteolytic halo was 2.915 ± 0.5017. Upon repression of *VMA2*, the relative size of the halo decreased to 1.639 ± 0.1371; this decrease was statistically significant compared to all three controls ($P < 0.01$). Because BSA media cannot be buffered to acidic pH without denaturing the BSA, we were unable to utilize growth-permissive media for these experiments. However, because the BSA medium utilized was not buffered to a specific pH (i.e., unbuffered) and tetR-*VMA2* grows similarly to the wild type on unbuffered media (Fig. 1), this defect likely is not due solely to slow growth by the tetR-*VMA2* strain under repressing conditions.

***VMA2* is involved in autophagy.** V-ATPase activity has previously been implicated in survival under conditions of nitrogen starvation (52); however, its exact role remains unclear (53). Therefore, we assessed the contribution of *VMA2* to long-term survival under conditions of nitrogen starvation using a 30-day assay to monitor resistance to nitrogen starvation (31). Because the growth of V-ATPase-deficient cells is pH sensitive, we measured the initial pH of the nitrogen starvation media (pH 4.5) and that over the course of the experiment. Periodic measurements of the medium pH in all treatments revealed no significant changes (pH 4.0 to 5.0; data not shown). The cells were grown in nitrogen starvation media with or without DOX for a period of 30 days, with samples taken at select time points for CFU counts. The THE1-CIp10 control strain with or without DOX and the tetR-*VMA2* strain without DOX exhibited a gradual decrease in CFU over the 30-day period (Fig. 8). However, repression of *VMA2* with DOX caused a dramatic decrease in CFU that persisted over the 30-day period (Fig. 8). Interestingly, while repression of *VMA2* impaired resistance to nitrogen starvation, it did not lead to complete cell death.

Survival of *C. albicans* under conditions of nitrogen starvation is accomplished via autophagic recycling of cellular material; therefore, resistance to nitrogen starvation is an indirect measure of autophagy (31). To confirm the role of *VMA2* in autophagy, we sought to monitor the fate of an autophagic marker. The hydrolase aminopeptidase I (Ape1) is encoded by the *C. albicans LAP41* gene (orf19.1628). Ape1p makes up the cytosol-to-vacuole targeting complex, which is engulfed by autophagosomes under starvation conditions (54, 55). Consequently, Ape1-GFP has been used commonly as an autophagic marker in *C. albicans* (31) and *S. cerevisiae* (55). Upon translation, the preform of Ape1 aggregates in the cytosol to form a homododecameric complex, also known as the cytosol-to-vacuole targeting (Cvt) complex. Under autophagic conditions, the Cvt complex is selectively shuttled to the vacuole by autophagosomes, where maturation of Ape1 occurs (54–56). Visualization of Ape1-GFP localization and processing upon nitrogen starvation can be used to identify defects in the autophagic pathway; Ape1-GFP originates in the cytosol and can be observed as intense fluorescent dots. Ape1-GFP then is trafficked to the vacuole, where it is visible first as intense spots and over time disperses throughout the vacuolar lumen as autophagosomes are degraded. We used a nourseothricin selection method to construct *C. albicans* strains, in both the THE1-CIp10 and tetR-*VMA2* backgrounds, in which the C terminus of Ape1p was tagged with GFP. The two anticipated localizations of Ape1-GFP (cytosol and vacuolar lumen) and its subsequent vacuolar dispersion were observed in THE1-CIp10 cells with or without DOX as well as tetR-*VMA2* cells without DOX 2 h after the transfer to nitrogen

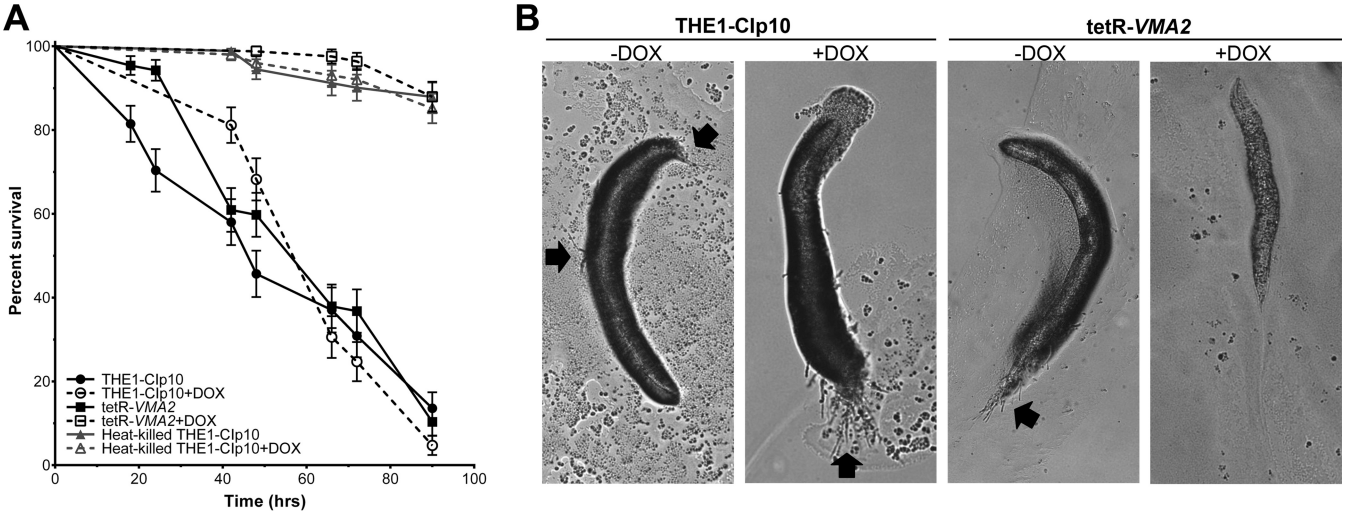

FIG 9 tetR-*VMA2* contribution to virulence in the *in vivo C. elegans* model. (A) Survival curve of nematodes infected with *C. albicans* strains THE1-CIp10 and tetR-*VMA2*, with and without DOX, or fed with heat-killed *C. albicans* THE1-CIp10 with and without DOX. Worm survival was monitored at select time points; worms that did not respond to stimulation with a platinum wire pick were scored as dead. Inhibition of *VMA2* leads to avirulence; survival of nematodes infected with DOX-repressed tetR-*VMA2* was not significantly different from survival of nematodes fed heat-killed *C. albicans* cells. (B) Light microscopy of nematodes infected with *C. albicans* strains. Black arrows indicate *C. albicans* hyphae piercing the *C. elegans* cuticle.

starvation media (Fig. 8B). We noted the presence of dispersed Ape1-GFP in all vacuoles, indicating active autophagic processes. In contrast, upon repression of *VMA2* with DOX in tetR-*VMA2* cells, intense spots of Ape1-GFP accumulated in the vacuole after 2 h (Fig. 8B). In THE1-CIp10 cells with or without DOX, the Ape1-GFP signal decreased from 2 h to 4 h (Fig. 8C). Without DOX, Ape1-GFP levels in tetR-*VMA2* cells were indistinguishable from those of the wild type (Fig. 8C). Unlike the control strains, Ape1-GFP remained present in vacuoles of the tetR-*VMA2* cells plus DOX after 4 h in nitrogen starvation media (Fig. 8C). At all time points, tetR-*VMA2* cells treated with DOX exhibited markedly higher levels of Ape1-GFP (Fig. 8B and C and data not shown). These data indicate a delay in autophagy upon repression of *VMA2*. Of note, a defined vacuolar compartment was no longer visible in tetR-*VMA2* cells treated with DOX past 24 h in nitrogen starvation media (data not shown). In contrast, an enlarged vacuolar compartment was clearly visible in control cells (both THE1-CIp10 with or without DOX and tetR-*VMA2* without DOX).

***VMA2* is required for virulence in an acidic infection model.** *C. albicans vma7*Δ, which is expected to lack all V-ATPase activity and exhibited the Vma$^-$ growth phenotype, is avirulent in a mouse model of systemic candidiasis (3). However, the pH-dependent phenotype of *vma* mutants makes interpretation of virulence models difficult, as in most model systems the physiological pH is restrictive for the growth of *vma* mutants. Therefore, we tested tetR-*VMA2* virulence in a *C. elegans* model of infection (34). *C. elegans* is an ideal organism for the study of virulence in *C. albicans vma* mutants, as the pH of the larynx and intestine of *C. elegans* nematodes, where *C. albicans* infection occurs (34, 35), ranges from 3.5 to 5.5 (57). For these studies, we analyzed infection at the permissive pH and temperature, under acidic pH conditions (pH 4.0) and at 30°C, because tetR-*VMA2* is unable to grow at neutral pH and low temperatures (i.e., 25°C). The wild-type worms were infected at 30°C and maintained at 30°C postinfection, with daily monitoring for survival. To ensure that neither high temperature (30°C) nor treatment with DOX were responsible for worm mortality, we included negative controls where worms were not infected with live *C. albicans* but rather were fed heat-killed *C. albicans* cells, which have been shown previously to be avirulent (34). Upon repression with DOX, tetR-*VMA2* exhibited attenuated virulence in the *C. elegans* model (Fig. 9A). Notably, survival of the worms infected with doxycycline-repressed tetR-*VMA2* was not significantly different from survival of untreated worms after 90 h (88.0% ± 3.6% survival for tetR-*VMA2* plus DOX compared to 87.9% ± 3.4% and 85.1% ± 3.5% survival for the negative controls with and without DOX, respectively). *C. elegans* nematodes were killed by infection with the THE1-CIp10 controls, with an LT_{50} of 66 h. Without DOX, nematode killing by the tetR-*VMA2* strain was not statistically significant ($P < 0.001$) compared to that of the THE1-CIp10 controls, with an LT_{50} of 66 h. In contrast, the LT_{50} of worms infected with the tetR-*VMA2* strain with DOX was 144 h, comparable to the negative-control nematodes fed heat-killed yeast. Further, worms scored as dead in the assay were subjected to analysis via light microscopy (Fig. 9B). Worms infected with THE1-CIp10 with or without DOX or tetR-*VMA2* without DOX cells had visible hyphae piercing the worm cuticle, indicative of hypha-mediated killing. In contrast, worms infected with DOX-repressed tetR-*VMA2* cells had no visible hyphal protrusions. We conclude that tetR-*VMA2* is avirulent in the acidic *C. elegans* infection model.

DISCUSSION

The contribution of several V-ATPase subunits to *C. albicans* cell biology and virulence has been studied previously (3, 4, 12, 13). Here, we present the study of *C. albicans VMA2*, which encodes the B subunit of the V-ATPase V_1 domain; this is the first component of the catalytic hexamer of the V_1 complex to be studied in depth in *C. albicans*. Repression of *VMA2* in *C. albicans* results in the Vma$^-$ phenotype, characterized by poor growth at alkaline pH and on nonfermentable carbon sources as well as reduced ability to respond to environmental stressors. This is in accord with pre-

vious studies of V-ATPase subunits encoded by a single gene in *C. albicans*, such as the V-ATPase structural genes *VMA7* and *VMA3* (3, 4). Genetic repression of *C. albicans VPH1* or *STV1*, which encode isoforms of the V-ATPase subunit V_oa, does not result in the Vma$^-$ phenotype (12, 13). As expected, repression of *VMA2* leads to complete inhibition of V-ATPase-specific (concanamycin A-sensitive) ATP hydrolysis and proton transport activities, similar to findings in studies of *VMA3* and *VPH1* (4, 12).

We previously studied susceptibility to fluconazole in a tetracycline-repressible *VMA3* strain and reported no difference in fluconazole susceptibility upon repression of *VMA3* (4). However, only one concentration of fluconazole was reported (5 μg/ml). Here, we extended those studies by testing both the tetR-*VMA2* and tetR-*VMA3* strains under a range of fluconazole concentrations (0.6125 to 10 μg/ml). Interestingly, repression of both *VMA2* and *VMA3* decreased *C. albicans* susceptibility to subinhibitory concentrations of fluconazole despite an overall impairment in the ability of these mutants to respond to stress. More than one possibility exists to explain this phenomenon. Upon repression of *VMA2* or *VMA3*, cells may compensate for V-ATPase loss by unknown mechanisms that may also lead to a decrease in the susceptibility to fluconazole. Alternatively, the dose-dependent antifungal activity of fluconazole may be directly attributable to effects on V-ATPase activity, as previously suggested (43). It is worth noting that null mutants of genes involved in ergosterol biosynthesis exhibit a similar decrease in fluconazole susceptibility (58, 59). The similar phenotype regarding fluconazole response in ergosterol and V-ATPase mutants further supports the notion that there is a link between V-ATPase and ergosterol.

Our phenotypic analyses of *VMA2* also revealed its contribution to filamentation on M199, YPD plus FCS, and RPMI media, but not to filamentation on Spider medium, even at acidic pH. Spider medium induces filamentation under conditions of carbon deprivation (28). These results are in contrast to those of our previous study of *VMA3*, which was unable to produce filaments on any medium tested, including Spider (4). It is conceivable that the V_o domain plays a role in filamentation under nutrient deprivation conditions; further work is required to address this possibility. This concept is supported by the fact that *S. cerevisiae vma2*Δ cells assemble V_o domains at the membrane but *vma3*Δ cells do not (60).

In addition to the differential contribution of *VMA2* and *VMA3* to filamentation under nutrient-poor conditions, the secretion of protease enzymes is also different following DOX-mediated suppression of *VMA2* and *VMA3*. Although inhibition of *VMA2* and *VMA3* completely abolished lipase secretion (4), only inhibition of *VMA3* fully impairs aspartyl protease secretion (4), whereas inhibition of *VMA2* results in a moderate decrease in aspartyl protease secretion. Notably, the V-ATPase V_o domain, but not V_1, has been shown previously to play a role in membrane fusion; SNARE complexes tether fusing membranes together, and the proteolipid ring of V-ATPase V_o complexes located on the vesicular membrane enlarges to create a fusion pore through which materials can flow (61). Our results could be explained if the V_o proteolipid ring and its involvement in membrane fusion are necessary for the secretion of aspartyl proteases but not lipases in *C. albicans*. Notably, we have shown that deletion of *VPH1*, a vacuolar isoform of V_oa that does not contribute to the V_o proteolipid ring, results in alkalinized vacuoles, complete elimination of lipase activity, and partial reduction of aspartyl protease activity (12) in a manner strikingly similar to that of *VMA2* repression. These overlapping results suggest that secretion of lipases depends on vacuolar acidification, whereas secretion of aspartyl proteases is maintained partially even in the presence of alkalinized vacuoles.

During both infection and colonization, *C. albicans* must survive robust oxidative stress conditions, and this ability to respond to oxidative stress previously has been correlated with virulence (62). Studies in *S. cerevisiae* V-ATPase mutants indicate that *vma* mutants cannot tolerate H_2O_2 and that the cells exhibit chronic oxidative stress (39). In the present study, we showed a role for *C. albicans* V-ATPase in response to oxidative stress, indicated by increased sensitivity to H_2O_2 upon repression of *VMA2* at acidic pH. This is a novel mechanism by which V-ATPase may contribute to virulence in *C. albicans*. Further studies are needed to clarify the exact role of V-ATPase in the *C. albicans* oxidative stress response pathway. Nonetheless, this finding emphasizes the multifactorial nature of the roles played by V-ATPase in fungal pathogenesis.

Autophagy is the process by which cells degrade cellular material in order to recycle cellular building blocks and is essential for survival under starvation conditions. Autophagy also is important for stress response, development and aging, and programmed cell death. In yeast, nutrient depletion in the cell causes a signaling cascade that induces autophagosome formation. The newly forming autophagosomal membrane elongates to enclose cellular components, such as cytoplasmic material, mitochondria, and nuclei. Autophagosomes then are transported to the vacuole and subsequently broken down. In *S. cerevisiae*, V-ATPase previously has been implicated in autophagic processes; V-ATPase mutants accumulate autophagosomes in the vacuole (52). In *C. albicans*, autophagy-deficient mutants are not impaired in filamentation or virulence in a mouse model of systematic infection (63, 64). However, autophagy has been implicated in survival within neutrophils and also may be important for commensalism by allowing long-term survival within the host (65). We showed that V-ATPase inhibition by repression of *VMA2* leads to defective autophagy, even under growth-permissive acidic conditions. Cells repressed for *VMA2* failed to survive nitrogen starvation and accumulated ApeI-GFP in the vacuole. Since the last step in autophagy is altered, our results suggest that lack of vacuolar acidification upon repression of *VMA2* is responsible for this effect.

V-ATPase is emerging as a potential antifungal target due to its far-reaching cellular importance (1, 5, 66). *C. albicans* V-ATPase mutants have been studied in mouse virulence models (3, 13). For example, *C. albicans vma7*Δ has reduced virulence, upholding the potential value of V-ATPase as a drug target (3). However, the pH-dependent growth of V-ATPase mutants can be a confounding factor in studies of V-ATPase and underlines the importance of studying phenotypes of interest under permissive pH conditions (pH 4.0 to 5.0) whenever possible. Whether reduced virulence is due merely to decreased growth at alkaline physiological pH rather than a role of V-ATPase in virulence-specific processes has remained unclear to date. Here, we present the first study of V-ATPase inhibition in an acidic model of infection. *Caenorhabditis elegans* is a soil-dwelling nematode that feeds on bacteria and fungi and is exposed *in situ* to a wide range of ingested pathogens (67). *C. elegans* is a useful system to study fungal pathogenesis due to its sophisticated, pathogen-specific immune system that includes immune response pathways conserved with mammals (34,

67–69). In fact, bacterial and fungal genes identified as important for pathogenesis in *C. elegans* infection assays have considerable overlap with genes previously identified as important for pathogenesis in mammalian infection models (69, 70). These characteristics underline the utility of *C. elegans* as a model host organism. In the *C. albicans*-*C. elegans* infection assay, *C. elegans* nematodes ingest *C. albicans* cells, which then persist within the *C. elegans* gastrointestinal tract and cause an infection. At this point, *C. elegans* immune defenses are induced, including fungus-specific transcriptional changes involving antimicrobial, secreted, or detoxification proteins (34). The infection culminates in *C. albicans* hyphae piercing the *C. elegans* cuticle and killing the worm (35). Because the *C. elegans* gastrointestinal tract and pharynx have very low pH, ranging from pH 5.5 in the pharynx to pH 3.5 in the lower intestine (57), *C. elegans* is an ideal model to study V-ATPase-mediated pathogenesis *in vivo*. We tested the contribution of *VMA2* to *C. albicans* virulence in an acidic environment, i.e., under pH conditions permissible for growth of V-ATPase-deficient cells. To establish this growth-permissive, acidic environment, we utilized both acidic media and an infection model where the site of infection is highly acidic. Upon repression of *VMA2*, the tetR-*VMA2* strain is avirulent. Therefore, we can conclude that the contributions of V-ATPase to stress responses, filamentation, and virulence are not attributable to its pH-dependent growth phenotype. Rather, intact V-ATPase function has a direct role in *C. albicans* pathogenesis. Ongoing studies in our laboratories to further elucidate the cell biology underpinning that role are in progress.

ACKNOWLEDGMENTS

We thank Hironobu Nakayama (Suzuka University of Medical Science, Japan) for providing strain THE1 and plasmid p99CAU1, Aaron P. Mitchell (Carnegie Mellon University) for providing plasmid pDDB57, Steven Bates (University of Exeter) for providing plasmid pGFP-NAT1, and Barbara Hunter (University of Texas Health Science Center at San Antonio) for assistance with transmission electron microscopy.

The *C. elegans* N2 strain and the *E. coli* OP50 strain were provided by the Caenorhabditis Genetics Center (CGC), which is funded by the NIH Office of Research Infrastructure Programs (P40 OD010440).

Sequence data for *C. albicans* were obtained from the Candida Genome Database. Sequencing of *C. albicans* was accomplished with the support of the NIDCR, NIH, and the Burroughs Wellcome Fund.

This work was supported by funding from the Department of Veterans' Affairs (Merit Award 5 I01 BX001130 to S.A.L.), Biomedical Research Institute of New Mexico (to S.A.L.), National Institutes of Health grant R01 GM086495 (to K.J.P.), UNM IDIP T32 institutional training grant NIH 5 T32 AI007538 (to S.M.B.), and National Institutes of Health grant K12 GM088021 (to S.R.H.).

REFERENCES

1. **Hayek SR, Lee SA, Parra KJ.** 2014. Advances in targeting the vacuolar proton-translocating ATPase (V-ATPase) for anti-fungal therapy. Front. Pharmacol. **5:**4. http://dx.doi.org/10.3389/fphar.2014.00004.
2. **Palmer GE, Kelly MN, Sturtevant JE.** 2005. The *Candida albicans* vacuole is required for differentiation and efficient macrophage killing. Eukaryot. Cell **4:**1677–1686. http://dx.doi.org/10.1128/EC.4.10.1677-1686.2005.
3. **Poltermann S, Nyugen M, Gunther J, Wendland J, Hartl A, Kunkel W, Zipfel PF, Eck R.** 2005. The putative vacuolar ATPase subunit Vma7p of *Candida albicans* is involved in vacuole acidification, hyphal development and virulence. Microbiology **151:**1645–1655. http://dx.doi.org/10.1099/mic.0.27505-0.
4. **Rane HS, Bernardo SM, Raines SM, Binder JL, Parra KJ, Lee SA.** 2013. *Candida albicans VMA3* is necessary for V-ATPase assembly and function and contributes to secretion and filamentation. Eukaryot. Cell **12:**1369–1382. http://dx.doi.org/10.1128/EC.00118-13.
5. **Parra KJ.** 2012. Vacuolar ATPase: a model proton pump for antifungal drug discovery, p 89–100. *In* Tegos G, Mylonakis E (ed), Antimicrobial drug discovery: emerging strategies. CAB International, Wallingford, England.
6. **Kane PM.** 2006. The where, when, and how of organelle acidification by the yeast vacuolar H+-ATPase. Microbiol. Mol. Biol. Rev. **70:**177–191. http://dx.doi.org/10.1128/MMBR.70.1.177-191.2006.
7. **Baars TL, Petri S, Peters C, Mayer A.** 2007. Role of the V-ATPase in regulation of the vacuolar fission-fusion equilibrium. Mol. Biol. Cell **18:**3873–3882. http://dx.doi.org/10.1091/mbc.E07-03-0205.
8. **Huang C, Chang A.** 2011. pH-dependent cargo sorting from the Golgi. J. Biol. Chem. **286:**10058–10065. http://dx.doi.org/10.1074/jbc.M110.197889.
9. **Tarsio M, Zheng H, Smardon AM, Martínez-Muñoz GA, Kane PM.** 2011. Consequences of loss of Vph1 protein-containing vacuolar ATPases (V-ATPases) for overall cellular pH homeostasis. J. Biol. Chem. **286:**28089–28096. http://dx.doi.org/10.1074/jbc.M111.251363.
10. **Martínez-Muñoz GA, Kane P.** 2008. Vacuolar and plasma membrane proton pumps collaborate to achieve cytosolic pH homeostasis in yeast. J. Biol. Chem. **283:**20309–20319. http://dx.doi.org/10.1074/jbc.M710470200.
11. **Perzov N, Nelson H, Nelson N.** 2000. Altered distribution of the yeast plasma membrane H+-ATPase as a feature of vacuolar H+-ATPase null mutants. J. Biol. Chem. **275:**40088–40095. http://dx.doi.org/10.1074/jbc.M007011200.
12. **Raines SM, Rane H, Bernardo SM, Binder JL, Lee SA, Parra KJ.** 2013. Deletion of V-ATPase Voa isoforms clarifies the role of vacuolar pH as a determinant of virulence-associated traits in *C. albicans*. J. Biol. Chem. **288:**6190–6201. http://dx.doi.org/10.1074/jbc.M112.426197.
13. **Patenaude C, Zhang Y, Cormack B, Köhler J, Rao R.** 2013. Essential role for vacuolar acidification in *Candida albicans* virulence. J. Biol. Chem. **288:**26256–26264. http://dx.doi.org/10.1074/jbc.M113.494815.
14. **Liu Q, Kane PM, Newman PR, Forgac M.** 1996. Site-directed mutagenesis of the yeast V-ATPase B subunit (Vma2p). J. Biol. Chem. **271:**2018–2022. http://dx.doi.org/10.1074/jbc.271.4.2018.
15. **Wilson RB, Davis D, Enloe BM, Mitchell AP.** 2000. A recyclable *Candida albicans URA3* cassette for PCR product-directed gene disruptions. Yeast **16:**65–70. http://dx.doi.org/10.1002/(SICI)1097-0061(20000115)16:1<65::AID-YEA508>3.0.CO;2-M.
16. **Bernardo SM, Lee SA.** 2010. *Candida albicans SUR7* contributes to secretion, biofilm formation, and macrophage killing. BMC Microbiol. **10:**133. http://dx.doi.org/10.1186/1471-2180-10-133.
17. **Wilson RB, Davis D, Mitchell AP.** 1999. Rapid hypothesis testing with *Candida albicans* through gene disruption with short homology regions. J. Bacteriol. **181:**1868–1874.
18. **Nakayama H, Mio T, Nagahashi S, Kokado M, Arisawa M, Aoki Y.** 2000. Tetracycline-regulatable system to tightly control gene expression in the pathogenic fungus *Candida albicans*. Infect. Immun. **68:**6712–6719. http://dx.doi.org/10.1128/IAI.68.12.6712-6719.2000.
19. **Bates S, Hughes HB, Munro CA, Thomas WPH, MacCallum DM, Bertram G, Atrih A, Ferguson MAJ, Brown AJP, Odds FC, Gow NAR.** 2006. Outer chain N-glycans are required for cell wall integrity and virulence of *Candida albicans*. J. Biol. Chem. **281:**90–98. http://dx.doi.org/10.1074/jbc.M510360200.
20. **Bernardo SM, Khalique Z, Kot J, Jones JK, Lee SA.** 2008. *Candida albicans VPS1* contributes to protease secretion, filamentation, and biofilm formation. Fungal Genet. Biol. **45:**861–877. http://dx.doi.org/10.1016/j.fgb.2008.01.001.
21. **Ramage G, López-Ribot JL.** 2005. Techniques for antifungal susceptibility testing of *Candida albicans* biofilms. Methods Mol. Med. **118:**71–79. http://dx.doi.org/10.1385/1-59259-943-5:071.
22. **Owegi MA, Pappas DL, Finch MW, Jr, Bilbo SA, Resendiz CA, Jacquemin LJ, Warrier A, Trombley JD, McCulloch KM, Margalef KLM, Mertz MJ, Storms JM, Damin CA, Parra KJ.** 2006. Identification of a domain in the V0 subunit d that is critical for coupling of the yeast vacuolar proton-translocating ATPase. J. Biol. Chem. **281:**30001–30014. http://dx.doi.org/10.1074/jbc.M605006200.
23. **Michel V, Licon-Munoz Y, Trujillo K, Bisoffi M, Parra KJ.** 2012. Inhibitors of vacuolar ATPase proton pumps inhibit human prostate cancer cell invasion and prostate-specific antigen expression and secretion. Int. J. Cancer **132:**E1–E10. http://dx.doi.org/10.1002/ijc.27811.
24. **Owegi MA, Carenbauer AL, Wick NM, Brown JF, Terhune KL, Bilbo**

SA, Weaver RS, Shircliff R, Newcomb N, Parra-Belky KJ. 2005. Mutational analysis of the stator subunit E of the yeast V-ATPase. J. Biol. Chem. **280:**18393–18402. http://dx.doi.org/10.1074/jbc.M412567200.
25. **Chan C-Y, Prudom C, Raines SM, Charkhzarrin S, Melman SD, De Haro LP, Allen C, Lee SA, Sklar LA, Parra KJ.** 2012. Inhibitors of V-ATPase proton transport reveal uncoupling functions of tether linking cytosolic and membrane domains of V0 subunit a (Vph1p). J. Biol. Chem. **287:**10236–10250. http://dx.doi.org/10.1074/jbc.M111.321133.
26. **Forgac M, Cantley L, Wiedenmann B, Altstiel L, Branton D.** 1983. Clathrin-coated vesicles contain an ATP-dependent proton pump. Proc. Natl. Acad. Sci. U. S. A. **80:**1300–1303. http://dx.doi.org/10.1073/pnas.80.5.1300.
27. **Perzov N, Padler-Karavani V, Nelson H, Nelson N.** 2002. Characterization of yeast V-ATPase mutants lacking Vph1p or Stv1p and the effect on endocytosis. J. Exp. Biol. **205:**1209–1219.
28. **Liu H, Köhler J, Fink GR.** 1994. Suppression of hyphal formation in *Candida albicans* by mutation of a *STE12* homolog. Science **266:**1723–1726. http://dx.doi.org/10.1126/science.7992058.
29. **Crandall M, Edwards JE, Jr.** 1987. Segregation of proteinase-negative mutants from heterozygous *Candida albicans*. J. Gen. Microbiol. **133:**2817–2824.
30. **Fu Y, Ibrahim AS, Fonzi W, Zhou X, Ramos CF, Ghannoum MA.** 1997. Cloning and characterization of a gene (*LIP1*) which encodes a lipase from the pathogenic yeast *Candida albicans*. Microbiology **14:**331–340.
31. **Palmer GE.** 2008. Autophagy in *Candida albicans*. Methods Enzymol. **451:**311–322. http://dx.doi.org/10.1016/S0076-6879(08)03221-7.
32. **Klionsky DJ, Abeliovich H, Agostinis P, Agrawal DK, Aliev G, Askew DS, Baba M, Baehrecke EH, Bahr BA, Ballabio A, Bamber BA, Bassham DC, Bergamini E, Bi X, Biard-Piechaczyk M, Blum JS, Bredesen DE, Brodsky JL, Brumell JH, Brunk UT, Bursch W, Camougrand N, Cebollero E, Cecconi F, Chen Y, Chin L-S, Choi A, Chu CT, Chung J, Clarke PGH, Clark RSB, Clarke SG, Clavé C, Cleveland JL, Codogno P, Colombo MI, Coto-Montes A, Cregg JM, Cuervo AM, Debnath J, Demarchi F, Dennis PB, Dennis PA, Deretic V, Devenish RJ, Di Sano F, Dice JF, Difiglia M, Dinesh-Kumar S, Distelhorst CW, Djavaheri-Mergny M, Dorsey FC, Dröge W, Dron M, Dunn WA, Jr, Duszenko M, et al.** 2008. Guidelines for the use and interpretation of assays for monitoring autophagy in higher eukaryotes. Autophagy **4:**151–175. http://dx.doi.org/10.4161/auto.5338.
33. **Milne SW, Cheetham J, Lloyd D, Aves S, Bates S.** 2011. Cassettes for PCR-mediated gene tagging in *Candida albicans* utilizing nourseothricin resistance. Yeast **28:**833–841. http://dx.doi.org/10.1002/yea.1910.
34. **Pukkila-Worley R, Ausubel FM, Mylonakis E.** 2011. *Candida albicans* infection of *Caenorhabditis elegans* induces antifungal immune defenses. PLoS Pathog. **7:**e1002074. http://dx.doi.org/10.1371/journal.ppat.1002074.
35. **Breger J, Fuchs BB, Aperis G, Moy TI, Ausubel FM, Mylonakis E.** 2007. Antifungal chemical compounds identified using a *C. elegans* pathogenicity assay. PLoS Pathog. **3:**e18. http://dx.doi.org/10.1371/journal.ppat.0030018.
36. **McMullen PD, Aprison EZ, Winter PB, Amaral LAN, Morimoto RI, Ruvinsky I.** 2012. Macro-level modeling of the response of *C. elegans* reproduction to chronic heat stress. PLoS Comput. Biol. **8:**e1002338. http://dx.doi.org/10.1371/journal.pcbi.1002338.
37. **Stiernagle T.** 11 February 2006. Maintenance of *C. elegans*, p 1–11. *In* WormBook: the online review of *C. elegans* biology. http://www.ncbi.nlm.nih.gov/books/NBK19649/.
38. **Sudbery PE.** 2011. Growth of *Candida albicans* hyphae. Nat. Rev. Microbiol. **9:**737–748. http://dx.doi.org/10.1038/nrmicro2636.
39. **Milgrom E, Diab H, Middleton F, Kane PM.** 2007. Loss of vacuolar proton-translocating ATPase activity in yeast results in chronic oxidative stress. J. Biol. Chem. **282:**7125–7136. http://dx.doi.org/10.1074/jbc.M608293200.
40. **De Dios CH, Román E, Monge RA, Pla J.** 2010. The role of MAPK signal transduction pathways in the response to oxidative stress in the fungal pathogen *Candida albicans*: implications in virulence. Curr. Protein Pept. Sci. **11:**693–703. http://dx.doi.org/10.2174/138920310794557655.
41. **Enjalbert B, MacCallum DM, Odds FC, Brown AJP.** 2007. Niche-specific activation of the oxidative stress response by the pathogenic fungus *Candida albicans*. Infect. Immun. **75:**2143–2151. http://dx.doi.org/10.1128/IAI.01680-06.
42. **Missall TA, Lodge JK, McEwen JE.** 2004. Mechanisms of resistance to oxidative and nitrosative stress: implications for fungal survival in mammalian hosts. Eukaryot. Cell **3:**835–846. http://dx.doi.org/10.1128/EC.3.4.835-846.2004.
43. **Zhang Y-Q, Gamarra S, Garcia-Effron G, Park S, Perlin DS, Rao R.** 2010. Requirement for ergosterol in V-ATPase function underlies antifungal activity of azole drugs. PLoS Pathog. **6:**e1000939. http://dx.doi.org/10.1371/journal.ppat.1000939.
44. **Gray KC, Palacios DS, Dailey I, Endo MM, Uno BE, Wilcock BC, Burke MD.** 2012. Amphotericin primarily kills yeast by simply binding ergosterol. Proc. Natl. Acad. Sci. U. S. A. **109:**2234–2239. http://dx.doi.org/10.1073/pnas.1117280109.
45. **Plant PJ, Manolson MF, Grinstein S, Demaurex N.** 1999. Alternative mechanisms of vacuolar acidification in H+-ATPase-deficient yeast. J. Biol. Chem. **274:**37270–37279. http://dx.doi.org/10.1074/jbc.274.52.37270.
46. **Bayer MJ, Reese C, Buhler S, Peters C, Mayer A.** 2003. Vacuole membrane fusion: V0 functions after trans-SNARE pairing and is coupled to the Ca2+-releasing channel. J. Cell Biol. **162:**211–222. http://dx.doi.org/10.1083/jcb.200212004.
47. **Strasser B, Iwaszkiewicz J, Michielin O, Mayer A.** 2011. The V-ATPase proteolipid cylinder promotes the lipid-mixing stage of SNARE-dependent fusion of yeast vacuoles. EMBO J. **30:**4126–4141. http://dx.doi.org/10.1038/emboj.2011.335.
48. **Vida TA, Emr SD.** 1995. A new vital stain for visualizing vacuolar membrane dynamics and endocytosis in yeast. J. Cell Biol. **128:**779–792. http://dx.doi.org/10.1083/jcb.128.5.779.
49. **Bastidas RJ, Heitman J, Cardenas ME.** 2009. The protein kinase Tor1 regulates adhesin gene expression in *Candida albicans*. PLoS Pathog. **5:**e1000294. http://dx.doi.org/10.1371/journal.ppat.1000294.
50. **Naglik JR, Challacombe SJ, Hube B.** 2003. *Candida albicans* secreted aspartyl proteinases in virulence and pathogenesis. Microbiol. Mol. Biol. Rev. **67:**400–428. http://dx.doi.org/10.1128/MMBR.67.3.400-428.2003.
51. **Calderone RA, Fonzi WA.** 2001. Virulence factors of *Candida albicans*. Trends Microbiol. **9:**327–335. http://dx.doi.org/10.1016/S0966-842X(01)02094-7.
52. **Nakamura N, Matsuura A, Wada Y, Ohsumi Y.** 1997. Acidification of vacuoles is required for autophagic degradation in the yeast, *Saccharomyces cerevisiae*. J. Biochem. **121:**338–344. http://dx.doi.org/10.1093/oxfordjournals.jbchem.a021592.
53. **Mijaljica D, Prescott M, Devenish RJ.** 2011. V-ATPase engagement in autophagic processes. Autophagy **7:**666–668. http://dx.doi.org/10.4161/auto.7.6.15812.
54. **Lynch-Day MA, Klionsky DJ.** 2010. The Cvt pathway as a model for selective autophagy. FEBS Lett. **584:**1359–1366. http://dx.doi.org/10.1016/j.febslet.2010.02.013.
55. **Suzuki K, Kamada Y, Ohsumi Y.** 2002. Studies of cargo delivery to the vacuole mediated by autophagosomes in *Saccharomyces cerevisiae*. Dev. Cell **3:**815–824. http://dx.doi.org/10.1016/S1534-5807(02)00359-3.
56. **Morales Quinones M, Winston JT, Stromhaug PE.** 2012. Propeptide of aminopeptidase 1 protein mediates aggregation and vesicle formation in cytoplasm-to-vacuole targeting pathway. J. Biol. Chem. **287:**10121–10133. http://dx.doi.org/10.1074/jbc.M111.311696.
57. **Chauhan VM, Orsi G, Brown A, Pritchard DI, Aylott JW.** 2013. Mapping the pharyngeal and intestinal pH of *Caenorhabditis elegans* and real-time luminal pH oscillations using extended dynamic range pH-sensitive nanosensors. ACS Nano **7:**5577–5587. http://dx.doi.org/10.1021/nn401856u.
58. **Jia N, Arthington-Skaggs B, Lee W, Pierson CA, Lees ND, Eckstein J, Barbuch R, Bard M.** 2002. *Candida albicans* sterol C-14 reductase, encoded by the *ERG24* gene, as a potential antifungal target site. Antimicrob. Agents Chemother. **46:**947–957. http://dx.doi.org/10.1128/AAC.46.4.947-957.2002.
59. **Sanglard D, Ischer F, Parkinson T, Falconer D, Bille J.** 2003. *Candida albicans* mutations in the ergosterol biosynthetic pathway and resistance to several antifungal agents. Antimicrob. Agents Chemother. **47:**2404–2412. http://dx.doi.org/10.1128/AAC.47.8.2404-2412.2003.
60. **Kane PM, Kuehn MC, Howald-Stevenson I, Stevens TH.** 1992. Assembly and targeting of peripheral and integral membrane subunits of the yeast vacuolar H(+)-ATPase. J. Biol. Chem. **267:**447–454.
61. **Peters C, Bayer MJ, Bühler S, Andersen JS, Mann M, Mayer A.** 2001. Trans-complex formation by proteolipid channels in the terminal phase of membrane fusion. Nature **409:**581–588. http://dx.doi.org/10.1038/35054500.

62. **Chauhan N, Latge J-P, Calderone R.** 2006. Signalling and oxidant adaptation in *Candida albicans* and *Aspergillus fumigatus*. Nat. Rev. Microbiol. **4:**435–444. http://dx.doi.org/10.1038/nrmicro1426.
63. **Palmer GE.** 2007. Autophagy in the invading pathogen. Autophagy **3:**251–253. http://dx.doi.org/10.4161/auto.3820.
64. **Palmer GE, Kelly MN, Sturtevant JE.** 2007. Autophagy in the pathogen *Candida albicans*. Microbiology **153:**51–58. http://dx.doi.org/10.1099/mic.0.2006/001610-0.
65. **Palmer GE, Askew DS, Williamson PR.** 2008. The diverse roles of autophagy in medically important fungi. Autophagy **4:**982–988. http://dx.doi.org/10.4161/auto.7075.
66. **Zhang Y, Rao R.** 2012. The V-ATPase as a target for antifungal drugs. Curr. Protein Pept. Sci. **13:**134–140. http://dx.doi.org/10.2174/138920312800493205.
67. **Schulenburg H, Kurz CL, Ewbank JJ.** 2004. Evolution of the innate immune system: the worm perspective. Immunol. Rev. **198:**36–58. http://dx.doi.org/10.1111/j.0105-2896.2004.0125.x.
68. **Irazoqui JE, Urbach JM, Ausubel FM.** 2010. Evolution of host innate defence: insights from *Caenorhabditis elegans* and primitive invertebrates. Nat. Rev. Immunol. **10:**47–58. http://dx.doi.org/10.1038/nri2689.
69. **Mylonakis E, Ausubel FM, Tang RJ, Calderwood SB.** 2003. The art of serendipity: killing of *Caenorhabditis elegans* by human pathogens as a model of bacterial and fungal pathogenesis. Expert Rev. Anti Infect. Ther. **1:**167–173. http://dx.doi.org/10.1586/14787210.1.1.167.
70. **Mylonakis E, Ausubel FM, Perfect JR, Heitman J, Calderwood SB.** 2002. Killing of *Caenorhabditis elegans* by *Cryptococcus neoformans* as a model of yeast pathogenesis. Proc. Natl. Acad. Sci. U. S. A. **99:**15675–15680. http://dx.doi.org/10.1073/pnas.232568599.